arXiv:1606.04144v1 [hep-ph] 13 Jun 2016

Higgs bosons production and decay at future e^+e^- linear colliders as a probe of the B-L model

F. Ramírez-Sánchez*,[1] A. Gutiérrez-Rodríguez†,[1] and M. A. Hernández-Ruíz‡[2]

[1] *Facultad de Física, Universidad Autónoma de Zacatecas*

Apartado Postal C-580, 98060 Zacatecas, México.

[2] *Unidad Académica de Ciencias Químicas, Universidad Autónoma de Zacatecas*

Apartado Postal C-585, 98060 Zacatecas, México.

(Dated: June 15, 2016)

Abstract

We study the phenomenology of the light and heavy Higgs boson production and decay in the context of a $U(1)_{B-L}$ extension of the Standard Model with an additional Z' boson at future e^+e^- linear colliders with center-of-mass energies of $\sqrt{s} = 500 - 3000\, GeV$ and integrated luminosities of $\mathcal{L} = 500 - 2000\, fb^{-1}$. The study includes the processes $e^+e^- \to (Z, Z') \to Zh$ and $e^+e^- \to (Z, Z') \to ZH$, considering both the resonant and non-resonant effects. We find that the total number of expected Zh and ZH events can reach 909,124 and 97,487, respectively, which is a very optimistic scenario and thus it would be possible to perform precision measurements for both Higgs bosons h and H, as well as for the Z' boson in future high-energy and high-luminosity e^+e^- colliders experiments. Our study complements other studies on the B-L model and on the Higgs-strahlung processes $e^+e^- \to (Z, Z') \to Zh$ and $e^+e^- \to (Z, Z') \to ZH$.

PACS numbers: 12.60.-i, 12.15.Mm, 13.66.Fg

Keywords: Models beyond the standard model, neutral currents, gauge and Higgs boson production in e^+e^- interactions.

* paco2357@yahoo.com.mx

† alexgu@fisica.uaz.edu.mx

‡ mahernan@uaz.edu.mx

I. INTRODUCTION

The $U(1)_{B-L}$ model [1–5] is one of the simplest extensions of the Standard Model (SM) with an extra $U(1)$ local gauge symmetry [6], where B and L represent the baryon number and lepton number, respectively. This B-L symmetry plays an important role in various physics scenarios beyond the SM: a) The gauge $U(1)_{B-L}$ symmetry group is contained in the Grand Unification Theory (GUT) described by a $SO(10)$ group [1]. b) The scale of the B-L symmetry breaking is related to the mass scale of the heavy right-handed Majorana neutrino mass terms and provide the well-known see-saw mechanism [7–11] to explain light left-handed neutrino mass. c) The B-L symmetry and the scale of its breaking are tightly connected to the baryogenesis mechanism through leptogenesis [12]. In addition, the model also contains an extra gauge boson Z' corresponding to B-L gauge symmetry and an extra SM singlet scalar (heavy Higgs boson H). This may change the SM phenomenology significantly and lead to interesting signatures at the current and future colliders such as the Large Hadron Collider (LHC) [13, 14], International Linear Collider (ILC) [15–20] and the Compact Linear Collider (CLIC) [21–23]. Therefore, another Higgs factory besides the LHC, such as the ILC and CLIC, which can study in detail and precisely determine the properties of the Higgs bosons h and H, is another important future step in high-energy and high-luminosity physics exploration.

The B-L model [24, 25] is attractive due to its relatively simple theoretical structure. The crucial test of the model is the detection of the new heavy neutral (Z') gauge boson and the new Higgs boson (H). The analysis of precision electroweak measurements indicates that the new Z' gauge boson should be heavier than about 1.2 TeV [26]. On the other hand, searches for both the heavy gauge boson (Z') and the additional heavy neutral Higgs boson (H) predicted by the B-L model are presently being conducted at the LHC. In this regard, the additional boson Z' of the B-L model has a mass which is given by the relation $M_{Z'} = 2v'g'_1$ [4, 5, 24, 25]. This boson Z' interacts with the leptons, quarks, heavy neutrinos and light neutrinos with interaction strengths proportional to the B-L gauge coupling g'_1. The Z' boson can be detected by observing di-leptonic and di-jet signals at colliders. The sensitivity limits on the mass $M_{Z'}$ of the boson Z' of the $U(1)_{B-L}$ model derived for the ATLAS and CMS collaborations are of the order of $\mathcal{O}(1.83 - 2.65)\, TeV$ [27–35]. In the case of the heavy neutral Higgs boson H of the B-L model, this can be produced at the high-

luminosity run at LHC (HL-LHC) through multiple production processes: gluon fusion, weak boson fusion, associated WH/ZH productions and the associated $t\bar{t}H$ production mode, with subsequent decay in heavy particles. The dominant decay modes are WW, hh and ZZ, respectively. In addition, the heavy Higgs H can also be produced in association with a Z' [4, 5]. The discovery prospects of the heavy neutral scalar H during the runs at HL-LHC are extensively studied in Refs. [4, 5, 36–38]. It is noteworthy that future LHC runs at 13-14 TeV could increase the Z' mass bounds to higher values, or evidence may be found of its existence. Precision studies of the Z' properties will require a new linear collider [39], which will allow us to perform precision studies of the Higgs sector. We refer the readers to Refs. [4, 5, 24, 25, 40–45] for a detailed description of the B-L model.

The Higgs-strahlung process $e^+e^- \to Zh$ [46–50] is one of the main production mechanisms of the Higgs boson in the future linear e^+e^- colliders such as the ILC and CLIC. Therefore, after the discovery of the Higgs boson, detailed experimental and theoretical studies are necessary for checking its properties and dynamics [51–54]. It is possible to search for the Higgs boson in the framework of the B-L model; however, the existence of a new gauge boson could also provide new Higgs particle production mechanisms that could prove its non-standard origin.

In this paper we study the phenomenology of Higgs bosons in the Type I see-saw model [7–11] of neutrino mass generation in presence of a spontaneously broken $U(1)_{B-L}$ symmetry at future electron-positron linear colliders such as the ILC and the CLIC. We consider both physical Higgs states emerging in the model, one of which is SM-like (h) while the other (H) is of B-L origin, both compliant with recent LHC data. We examine a variety of h, H decay channels while we concentrate on the $e^+e^- \to Zh$ and ZH production modes, including the possibility of Z' mediation, which could be resonant, as we allow for Z/Z' mixing (in presence of relevant experimental constraints from LEP).

It is worth mentioning that in Ref. [40], the authors made a very exhaustive study of Higgs physics through the Higgs-strahlung processes $e^+e^- \to Z'h, Z'H$, the associated production of a Higgs boson and a pair top quark $e^+e^- \to t\bar{t}h, t\bar{t}H$ and the associated production of a Higgs boson pair and a Z' boson $e^+e^- \to hhZ'$ in the aforementioned B-L model at future e^+e^- linear colliders. They do not consider, however, the case of Z/Z' mixing. Furthermore, Ref. [40] is primarily a numerical analysis, whereas in the present paper we present a wealth of useful analytical formulae. In addition, our analytical and numerical results for the Higgs

bosons production and decay at future e^+e^- colliders are helpful in searching for signatures of new physics and could be of scientific significance. Moreover, our study complements others studies on the B-L model and on the Higgs-strahlung processes $e^+e^- \to (Z, Z') \to Zh$ and $e^+e^- \to (Z, Z') \to ZH$, respectively.

The different stages of high-energy and high-luminosity of the ILC and the CLIC would provide a clean environment to study the properties of additional Z' and Higgs bosons through the production of a Z/Z' in association with a Higgs boson which is SM-like (h), while the other (H) is of B-L origin. The different Higgs boson production processes where the signatures can best be exploited to reveal the B-L nature of the electroweak symmetry breaking (EWSB) and in association with heavy particles, both SM (W, Z bosons and t (anti)quarks) and B-L (Z' boson and ν_R neutrinos), are $e^+e^- \to Zh, ZH, Z'h, Z'H$ (Higgs-strahlung process), $e^+e^- \to \nu_e\bar{\nu}_e h$ (WW vector boson fusion process) and $e^+e^- \to e^+e^-h$ (ZZ vector boson fusion process). Other important Higgs boson production mechanisms via a Z' boson which are also accessible to ILC and CLIC, are $e^+e^- \to t\bar{t}h, t\bar{t}H$ and $e^+e^- \to Zhh, Z'hh$, where the processes $e^+e^- \to t\bar{t}h, t\bar{t}H$, will play an important role for the precision measurements of the top Yukawa coupling, while the processes $e^+e^- \to Zhh, Z'hh$ will be crucial to understand the Higgs self-coupling and the mechanism of EWSB and mass generation. The Higgs self-coupling can be a non-trivial probe of the Higgs potential and probably the most decisive test of the EWSB mechanism. Detailed discussions on these processes and some new physics models can be found in Refs. [18, 19, 22, 55, 56].

Although we do not consider the background of the processes that we study, it is worth mentioning that the most important background of the processes studied in our article, $e^+e^- \to Zh$ and ZH, are: $ZZ, Z\gamma, \gamma\gamma$ for the b-quark final state ($e^+e^- \to Zh \to e^+e^-b\bar{b}, \mu^+\mu^-b\bar{b}$) and W^+W^-Z/γ for the W-boson final state ($e^+e^- \to Zh \to e^+e^-W^+W^-, \mu^+\mu^-W^+W^-$), respectively [18, 19, 22, 55, 56].

As mentioned above, our aim in the present paper is to study the phenomenology of the light and heavy Higgs boson production and decay, as well as the sensitivity of the Z' boson of the B-L model as a source of Higgs bosons through the Higgs-strahlung processes $e^+e^- \to (Z, Z') \to Zh$ and $e^+e^- \to (Z, Z') \to ZH$, including both the resonant and non-resonant effects at future high-energy and high-luminosity linear e^+e^- colliders. We evaluate the total cross section for Zh and ZH production and we calculate the total number of events for integrated luminosities of $\mathcal{L} = 500 - 2000\, fb^{-1}$ and center-of-mass energies of

$\sqrt{s} = 500 - 3000\,GeV$. We find that the total number of expected Zh and ZH events for the e^+e^- colliders is very promising and that it would be possible to perform precision measurements for both Higgs bosons h and H, as well as for the Z' boson.

This paper is organized as follows. In Section II, we present the B-L theoretical model. In Section III, we present the decay widths of the Z' heavy gauge boson of the B-L model. In Section IV, we present the calculation of the cross section for the process $e^+e^- \to (Z, Z') \to Zh$. In Section V, we present the decay widths of the H heavy Higgs boson of the B-L model. In Section VI, we present the calculation of the cross section for the process $e^+e^- \to (Z, Z') \to ZH$, and finally, we present our results and conclusions in Section VII.

II. BRIEF REVIEW OF THE B-L THEORETICAL MODEL

The solid evidence for the non-vanishing neutrino masses has been confirmed by various neutrino oscillation phenomena and indicates the evidence of new physics beyond the SM. In the SM, neutrinos are massless due to the absence of right-handed neutrinos and the exact B-L conservation. The most attractive idea to naturally explain the tiny neutrino masses is the seesaw mechanism [8–10, 57], in which the right-handed (RH) neutrinos singlet under the SM gauge group is introduced. The gauged $U(1)_{B-L}$ model based on the gauge group $SU(3)_C \times SU(2)_L \times U(1)_Y \times U(1)_{B-L}$ [7, 58] is an elegant and simple extension of the SM in which the RH heavy neutrinos are essential both for anomaly cancelation and preserving gauge invariance. In addition, the mass of RH neutrinos arises associated with the $U(1)_{B-L}$ gauge symmetry breaking. Therefore, the fact that neutrinos are massive indicates that the SM requires extension.

We consider a $SU(3)_C \times SU(2)_L \times U(1)_Y \times U(1)_{B-L}$ model, which is one of the simplest extensions of the SM [4, 5, 7, 24, 40–45, 58], where $U(1)_{B-L}$, represents the additional gauge symmetry. The gauge invariant Lagrangian of this model is given by

$$\mathcal{L} = \mathcal{L}_s + \mathcal{L}_{YM} + \mathcal{L}_f + \mathcal{L}_Y, \tag{1}$$

where $\mathcal{L}_s, \mathcal{L}_{YM}, \mathcal{L}_f$ and $\mathcal{L}_Y$ are the scalar, Yang-Mills, fermion and Yukawa sector, respectively.

The model consists of one doublet Φ and one singlet χ and we briefly describe the la-

grangian including the scalar, fermion and gauge sector, respectively. The Lagrangian for the gauge sector is given by [4, 44, 59, 60],

$$\mathcal{L}_g = -\frac{1}{4}B_{\mu\nu}B^{\mu\nu} - \frac{1}{4}W^a_{\mu\nu}W^{a\mu\nu} - \frac{1}{4}Z'_{\mu\nu}Z'^{\mu\nu}, \tag{2}$$

where $W^a_{\mu\nu}$, $B_{\mu\nu}$ and $Z'_{\mu\nu}$ are the field strength tensors for $SU(2)_L$, $U(1)_Y$ and $U(1)_{B-L}$, respectively.

The Lagrangian for the scalar sector of the model is

$$\mathcal{L}_s = (D^\mu\Phi)^\dagger(D_\mu\Phi) + (D^\mu\chi)^\dagger(D_\mu\chi) - V(\Phi,\chi), \tag{3}$$

where the potential term is [42],

$$V(\Phi,\chi) = m^2(\Phi^\dagger\Phi) + \mu^2|\chi|^2 + \lambda_1(\Phi^\dagger\Phi)^2 + \lambda_2|\chi|^4 + \lambda_3(\Phi^\dagger\Phi)|\chi|^2, \tag{4}$$

with Φ and χ as the complex scalar Higgs doublet and singlet fields, respectively. The covariant derivative is given by [40–42]

$$D_\mu = \partial_\mu + ig_s t^\alpha G^\alpha_\mu + i[gT^a W^a_\mu + g_1 Y B_\mu + (\tilde{g}Y + g'_1 Y_{B-L})B'_\mu], \tag{5}$$

where g_s, g, g_1 and g'_1 are the $SU(3)_C$, $SU(2)_L$, $U(1)_Y$ and $U(1)_{B-L}$ couplings with t^α, T^a, Y and Y_{B-L} being their respective group generators. The mixing between the two Abelian groups is described by the new coupling $\tilde{g}$. The electromagnetic charges on the fields are the same as those of the SM and the Y_{B-L} charges for quarks, leptons and the scalar fields are given by: $Y^{\text{quarks}}_{B-L} = 1/3$, $Y^{\text{leptons}}_{B-L} = -1$ with no distinction between generations for ensuring universality, $Y_{B-L}(\Phi) = 0$ and $Y_{B-L}(\chi) = 2$ [4, 5, 40–42] to preserve the gauge invariance of the model, respectively.

An effective coupling and effective charge such as g' and Y' are usually introduced as $g'Y' = \tilde{g}Y + g'_1 Y_{B-L}$ and some specific benchmark models [61, 62] can be recovered by particular choices of both $\tilde{g}$ and g'_1 gauge couplings at a given scale, generally the electroweak scale. For instance, the pure B-L model is obtain by the condition $\tilde{g} = 0$ ($Y' = Y_{B-L}$) which implies the absence of mixing at the electroweak scale. Other benchmark models of the general parameterisation are the Sequential Standar Model (SSM), the $U(1)_R$ model and the $U(1)_\chi$ model. The SSM is reproduced by the condition $g'_1 = 0$ ($Y' = Y$), and the $U(1)_R$

extension is realised by the condition $\tilde{g} = -2g_1'$, while the $SO(10)$-inspired $U(1)_\chi$ model is described by $\tilde{g} = -\frac{4}{5}g_1'$.

The doublet and singlet scalars are

$$\Phi = \begin{pmatrix} G^{\pm} \\ \frac{v+\phi^0+iG_Z}{\sqrt{2}} \end{pmatrix}, \qquad \chi = \left(\frac{v' + \phi'^0 + iz'}{\sqrt{2}}\right), \tag{6}$$

with $G^{\pm}$, G_Z and z' the Goldstone bosons of $W^{\pm}$, Z and Z', respectively, while $v \approx 246\,GeV$ is the electroweak symmetry breaking scale and v' is the B-L symmetry breaking scale constrained by the electroweak precision measurement data whose value is assumed to be of the order TeV.

After spontaneous symmetry breaking, the two scalar fields can be written as,

$$\Phi = \begin{pmatrix} 0 \\ \frac{v+\phi^0}{\sqrt{2}} \end{pmatrix}, \qquad \chi = \frac{v' + \phi'^0}{\sqrt{2}}, \tag{7}$$

with v and v' real and positive. Minimization of Eq. (4) gives

$$\begin{aligned} m^2 + 2\lambda_1 v^2 + \lambda_3 v v' &= 0, \\ \mu^2 + 4\lambda_2 v'^2 + \lambda_3 v v' &= 0. \end{aligned} \tag{8}$$

To compute the scalar masses, we must expand the potential in Eq. (4) around the minima in Eq. (7). Using the minimization conditions, we have the following scalar mass matrix:

$$\mathcal{M} = \begin{pmatrix} \lambda_1 v^2 & \frac{\lambda_3 v v'}{2} \\ \frac{\lambda_3 v v'}{2} & \lambda_2 v'^2 \end{pmatrix} = \begin{pmatrix} \mathcal{M}_{11} & \mathcal{M}_{12} \\ \mathcal{M}_{21} & \mathcal{M}_{22} \end{pmatrix}. \tag{9}$$

The expressions for the scalar mass eigenvalues ($M_H > M_h$) are

$$M^2_{H,h} = \frac{(\mathcal{M}_{11} + \mathcal{M}_{22}) \pm \sqrt{(\mathcal{M}_{11} - \mathcal{M}_{22})^2 + 4\mathcal{M}_{12}^2}}{2}, \tag{10}$$

and the mass eigenstates are linear combinations of ϕ^0 and ϕ'^0, and written as,

$$\begin{pmatrix} h \\ H \end{pmatrix} = \begin{pmatrix} \cos\alpha & -\sin\alpha \\ \sin\alpha & \cos\alpha \end{pmatrix} \begin{pmatrix} \phi^0 \\ \phi'^0 \end{pmatrix}, \tag{11}$$

where h is the SM-like Higgs boson, H is an extra Higgs boson and the scalar mixing angle α ($-\frac{\pi}{2} \leq \alpha \leq \frac{\pi}{2}$) can be expressed as

$$\tan(2\alpha) = \frac{2\mathcal{M}_{12}}{\mathcal{M}_{22} - \mathcal{M}_{11}} = \frac{\lambda_3 v v'}{\lambda_2 v'^2 - \lambda_1 v^2}, \tag{12}$$

while coupling constants λ_1, λ_2 and λ_3 are determined using Eqs. (10)-(12):

$$\begin{aligned} \lambda_1 &= \frac{M_H^2}{4v^2}(1-\cos 2\alpha) + \frac{M_h^2}{4v^2}(1+\cos 2\alpha), \\ \lambda_2 &= \frac{M_h^2}{4v'^2}(1-\cos 2\alpha) + \frac{M_H^2}{4v'^2}(1+\cos 2\alpha), \\ \lambda_3 &= \sin 2\alpha(\frac{M_H^2 - M_h^2}{2vv'}). \end{aligned} \tag{13}$$

If the LHC data [63, 64] are interpreted by identifying h with the recently observed Higgs boson, then the scalar mixing angle α should satisfy the constraint $\sin^2\alpha \lesssim 0.33(0.36)$ for $M_H = 200(300)\,GeV$ as discussed in [65–67].

In Table I, the interactions of h and H with the fermions, gauge bosons, scalar and scalar self-interactions are expressed in terms of the parameters of the B-L model.

To determine the mass spectrum of the gauge bosons, we have to expand the scalar kinetic terms as with the SM. We expect that there exists a massless gauge boson, the photon, while the other gauge bosons become massive. The extension we are studying is in the Abelian sector of the SM gauge group, so that the charged gauge bosons $W^{\pm}$ will have masses given by their SM expressions related to the $SU(2)_L$ factor only. The other gauge boson masses are not so simple to identify because of mixing. In fact, analogous to the SM, the fields of definite mass are linear combinations of B^μ, W_3^μ and B'^μ, the relation between the neutral gauge bosons (B^μ, W_3^μ and B'^μ) and the corresponding mass eigenstates is given by [24, 25, 40, 41]

$$\begin{pmatrix} B^\mu \\ W^{3\mu} \\ B'^\mu \end{pmatrix} = \begin{pmatrix} \cos\theta_W & -\sin\theta_W\cos\theta_{B-L} & \sin\theta_W\sin\theta_{B-L} \\ \sin\theta_W & \cos\theta_W\cos\theta_{B-L} & -\cos\theta_W\sin\theta_{B-L} \\ 0 & \sin\theta_{B-L} & \cos\theta_{B-L} \end{pmatrix} \begin{pmatrix} A^\mu \\ Z^\mu \\ Z'^\mu \end{pmatrix}, \tag{14}$$

with $-\frac{\pi}{4} \leq \theta_{B-L} \leq \frac{\pi}{4}$, such that

$$\tan 2\theta_{B-L} = \frac{2\tilde{g}\sqrt{g^2+g_1^2}}{\tilde{g}^2+16(\frac{v'}{v})^2 g_1'^2 - g^2 - g_1^2}, \tag{15}$$

and the mass spectrum of the gauge bosons is given by

$$\begin{aligned}
M_\gamma &= 0, \\
M_{W^\pm} &= \frac{1}{2}vg, \\
M_Z &= \frac{v}{2}\sqrt{g^2+g_1^2}\sqrt{\frac{1}{2}\Big(\frac{\tilde{g}^2+16(\frac{v'}{v})^2 g_1'^2}{g^2+g_1^2}+1\Big) - \frac{\tilde{g}}{\sin 2\theta_{B-L}\sqrt{g^2+g_1^2}}}, \\
M_{Z'} &= \frac{v}{2}\sqrt{g^2+g_1^2}\sqrt{\frac{1}{2}\Big(\frac{\tilde{g}^2+16(\frac{v'}{v})^2 g_1'^2}{g^2+g_1^2}+1\Big) + \frac{\tilde{g}}{\sin 2\theta_{B-L}\sqrt{g^2+g_1^2}}},
\end{aligned} \tag{16}$$

where M_Z and $M_{W^\pm}$ are the SM gauge bosons masses and $M_{Z'}$ is the mass of new neutral gauge boson Z', which strongly depends on v' and g_1'. For $\tilde{g} = 0$, there is no mixing between the new and SM gauge bosons Z' and Z. In this case, the $U(1)_{B-L}$ model is called the pure or minimal model $U(1)_{B-L}$. In this article we consider the case $\tilde{g} \neq 0$, which is mostly determined by the other gauge couplings g_1 and g_1' [65–67]. The electroweak precision measurement data can give stringent constraints on the $Z - Z'$ mixing angle θ_{B-L} expressed in Eq. (15) [68].

In the Lagrangian of the $SU(3)_C \times SU(2)_L \times U(1)_Y \times U(1)_{B-L}$ model, the terms for the interactions between neutral gauge bosons Z, Z' and a pair of fermions of the SM can be written in the form [4, 5, 69–71]

$$\mathcal{L}_{NC} = \frac{-ig}{\cos\theta_W}\sum_f \bar{f}\gamma^\mu \frac{1}{2}(g_V^f - g_A^f\gamma^5) f Z_\mu + \frac{-ig}{\cos\theta_W}\sum_f \bar{f}\gamma^\mu \frac{1}{2}(g_V'^f - g_A'^f\gamma^5) f Z'_\mu. \tag{17}$$

From this Lagrangian we determine the expressions for the new couplings of the Z, Z' bosons with the SM fermions, which are given in Table II. The couplings g_V^f ($g_V'^f$) and g_A^f ($g_A'^f$) depend on the $Z - Z'$ mixing angle θ_{BL} and the coupling constant g_1' of the B-L interaction. In these couplings, the current bound on the mixing angle is $|\theta_{BL}| \leq 10^{-3}$ [72]. In the decoupling limit, when $\theta_{BL} = 0$ and $g_1' = 0$, the couplings of the SM are recovered.

TABLE I: Fermion, vector boson, scalar coupling and scalar self-interactions in the B-L model.

Particle	Couplings
$f\bar{f}h$	$g_{f\bar{f}h} = i\frac{M_f}{v}\sin\alpha$
$f\bar{f}H$	$g_{f\bar{f}H} = i\frac{M_f}{v}\cos\alpha$
$Z_\mu Z_\nu h$	$g_{ZZh} = -i\frac{2M_Z^2}{v}g_{\mu\nu}\cos\alpha$
$Z_\mu Z_\nu H$	$g_{ZZH} = -i\frac{2M_Z^2}{v}g_{\mu\nu}\sin\alpha$
$W_\mu^- W_\nu^+ h$	$g_{W^-W^+h} = i\frac{eM_W}{\sin\theta_W}g_{\mu\nu}\cos\alpha$
$W_\mu^- W_\nu^+ H$	$g_{W^-W^+H} = i\frac{eM_W}{\sin\theta_W}g_{\mu\nu}\sin\alpha$
$Z_\mu Z'_\nu h$	$g_{ZZ'h} = 2i[\frac{1}{4}v\cos\alpha f(\theta_{BL}, g'_1) - v'\sin\alpha g(\theta_{BL}, g'_1)]g_{\mu\nu}$, $f(\theta_{BL}, g'_1) = -\sin(2\theta')(g_1^2 + g_2^2 + g_1'^2) - 2\cos(2\theta')g_1\sqrt{g_1^2 + g_2^2}$, $g(\theta_{BL}, g'_1) = \frac{1}{4}\sin(2\theta')g_1'^2$.
$Z_\mu Z'_\nu H$	$g_{ZZ'H} = 2i[\frac{1}{4}v\sin\alpha f(\theta_{BL}, g'_1) + v'\cos\alpha g(\theta_{BL}, g'_1)]g_{\mu\nu}$,
$W_\mu^-(p_1)W_\nu^+(p_2)Z_\rho(p_3)$	$g_{W^-W^+Z} = -ig\cos\theta_W\cos\theta_{B-L}[(p_1-p_2)_\rho g_{\mu\nu} + (p_2-p_3)_\mu g_{\nu\rho} + (p_3-p_1)_\nu g_{\rho\nu}]$,
$W_\mu^-(p_1)W_\nu^+(p_2)Z'_\rho(p_3)$	$g_{W^-W^+Z'} = -ig\cos\theta_W\sin\theta_{B-L}[(p_1-p_2)_\rho g_{\mu\nu} + (p_2-p_3)_\mu g_{\nu\rho} + (p_3-p_1)_\nu g_{\rho\nu}]$,
$Z'_\mu Z'_\nu h$	$g_{Z'Z'h} = -8\sin\alpha g_1'^2 v' g_{\mu\nu}$
$Z'_\mu Z'_\nu H$	$g_{Z'Z'H} = -8\cos\alpha g_1'^2 v' g_{\mu\nu}$
$\nu_R\bar{\nu}_R h$	$g_{\nu_R\bar{\nu}_R h} = -i\frac{M_{\nu_R}}{v'}\sin\alpha$
$\nu_R\bar{\nu}_R H$	$g_{\nu_R\bar{\nu}_R H} = i\frac{M_{\nu_R}}{v'}\cos\alpha$
hhh	$g_{hhh} = \frac{1}{4}\lambda_1 v(3\cos\alpha + \cos 3\alpha) + \frac{1}{4}\lambda_2 v'(-3\sin\alpha + \sin 3\alpha)$ $+\frac{1}{8}\lambda_3[v(\cos\alpha - \cos 3\alpha) - v'(\sin\alpha + \sin 3\alpha)]$
hhH	$g_{hhH} = 3\lambda_1 v(\cos^2\alpha\sin\alpha) + 3\lambda_2 v'(\cos\alpha\sin^2\alpha)$ $+\frac{1}{8}\lambda_3[v'(\cos\alpha + 3\cos 3\alpha) + v(\sin\alpha - 3\sin 3\alpha)]$

III. THE DECAY WIDTHS OF THE Z' BOSON IN THE B-L MODEL

In this section we present the decay widths of the Z' boson [26, 69, 73–75] in the context of the B-L model needed in the calculation of the cross section for the Higgs-strahlung process $e^+e^- \to Zh$. The decay width of the Z' boson to fermions is given by

TABLE II: The new couplings of the Z, Z' bosons with the SM fermions. $g = e/\sin\theta_W$ and θ_{BL} is the $Z - Z'$ mixing angle.

Particle	Couplings
$f\bar{f}Z$	$g_V^f = T_3^f \cos\theta_{BL} - 2Q_f \sin^2\theta_W \cos\theta_{BL} + \frac{2g_1'}{g}\cos\theta_W \sin\theta_{BL}$, $g_A^f = T_3^f \cos\theta_{BL}$.
$f\bar{f}Z'$	$g_V^{'f} = -T_3^f \sin\theta_{BL} - 2Q_f \sin^2\theta_W \sin\theta_{BL} + \frac{2g_1'}{g}\cos\theta_W \cos\theta_{BL}$, $g_A^{'f} = -T_3^f \sin\theta_{BL}$.

$$\Gamma(Z' \to f\bar{f}) = \frac{2G_F}{3\pi\sqrt{2}} N_c M_Z^2 M_{Z'} \sqrt{1 - \frac{4M_f^2}{M_{Z'}^2}} \left[(g_V'^f)^2 \left\{ 1 + 2\left(\frac{M_f^2}{M_{Z'}^2}\right)\right\} + (g_A'^f)^2 \left\{ 1 - 4\left(\frac{M_f^2}{M_{Z'}^2}\right)\right\}\right], \tag{18}$$

where N_c is the color factor ($N_c = 1$ for leptons, $N_c = 3$ for quarks) and the couplings $g_V'^f$ and $g_A'^f$ of the Z' boson with the SM fermions are given in Table II.

The decay width of the Z' boson to heavy neutrinos is

$$\Gamma(Z' \to \nu_R \bar{\nu}_R) = \frac{g_1^{'2}}{24\pi} \sin^2\theta_{BL} M_{Z'} \sqrt{1 - \frac{4M_{\nu_R}^2}{M_{Z'}^2}} \left[1 - \frac{4M_{\nu_R}^2}{M_{Z'}^2}\right], \tag{19}$$

where the width given by Eq. (19) implies that the right-handed neutrino must be lighter than half the Z' mass, $M_{\nu_R} < \frac{M_{Z'}}{2}$, and the conditions under which this inequality holds is for coupled heavy neutrinos, i.e. with minor mass less than $\frac{M_{Z'}}{2}$. The possibility of the Z' heavy boson decaying into pairs of heavy neutrinos is certainty one of the most interesting of its features.

The Z' partial decay widths involving vector bosons and the scalar bosons are

$$\Gamma(Z' \to W^+W^-) = \frac{G_F M_W^2}{24\pi\sqrt{2}} \cos^2\theta_W \sin^2\theta_{BL} M_{Z'} \left(\frac{M_{Z'}}{M_Z}\right)^4 \sqrt{\left(1 - 4\frac{M_W^2}{M_{Z'}^2}\right)^3} \left[1 + 20\frac{M_W^2}{M_{Z'}^2} + 12\frac{M_W^4}{M_{Z'}^4}\right], \tag{20}$$

$$\Gamma(Z' \to Zh) = \frac{G_F M_Z^2 M_{Z'}}{24\pi\sqrt{2}} \sqrt{\lambda_h} \left[\lambda_h + 12\frac{M_Z^2}{M_{Z'}^2}\right] \left[f(\theta_{BL}, g_1') \cos\alpha + g(\theta_{BL}, g_1') \sin\alpha \right]^2, \tag{21}$$

$$\Gamma(Z' \to ZH) = \frac{G_F M_Z^2 M_{Z'}}{24\pi\sqrt{2}}\sqrt{\lambda_H}\Big[\lambda_H + 12\frac{M_Z^2}{M_{Z'}^2}\Big]\Big[f(\theta_{BL}, g_1')\sin\alpha - g(\theta_{BL}, g_1')\cos\alpha\Big]^2, \quad (22)$$

where

$$\begin{aligned}
\lambda_{h,H}\Big(1, \frac{M_Z^2}{M_{Z'}^2}, \frac{M_{h,H}^2}{M_{Z'}^2}\Big) &= 1 + \Big(\frac{M_Z^2}{M_{Z'}^2}\Big)^2 + \Big(\frac{M_{h,H}^2}{M_{Z'}^2}\Big)^2 - 2\Big(\frac{M_Z^2}{M_{Z'}^2}\Big) - 2\Big(\frac{M_{h,H}^2}{M_{Z'}^2}\Big) - 2\Big(\frac{M_Z^2}{M_{Z'}^2}\Big)\Big(\frac{M_{h,H}^2}{M_{Z'}^2}\Big), \\
f(\theta_{BL}, g_1') &= \Big(1 + \frac{v^2 g_1'^2}{4M_Z^2}\Big)\sin(2\theta_{BL}) + \Big(\frac{v g_1'}{M_Z}\Big)\cos(2\theta_{BL}), \quad (23) \\
g(\theta_{BL}, g_1') &= \Big(\frac{vv'}{4M_Z^2}\Big) g_1'^2 \sin(2\theta_{BL}).
\end{aligned}$$

In the BL model, the heavy gauge boson mass $M_{Z'}$ satisfies the relation $M_{Z'} = 2v'g_1'$ [4, 5, 24, 25, 40, 41], and considering the most recent limit from $\frac{M_{Z'}}{g_1'} \geq 6.9\,TeV$ [62, 76, 77], it is possible to obtain a direct bound on the B-L breaking scale v'. In our next numerical calculation, we will take $v' = 3.45\,TeV$, while $\alpha = \frac{\pi}{9}$ for the $h - H$ mixing angle in correspondence with Refs. [4, 13, 14, 78].

IV. THE HIGGS-STRAHLUNG PROCESS $e^+e^- \to Zh$ IN THE B-L MODEL

In this section, we calculate the Higgs production cross section via the Higgs-strahlung process $e^+e^- \to Zh$ in the context of the B-L model at future high-energy and high-luminosity linear electron-positron colliders, such as the ILC and CLIC.

The Feynman diagrams contributing to the process $e^+e^- \to (Z, Z') \to Zh$ are shown in Fig. 1. The respective transition amplitudes are thus given by

$$\mathcal{M}_Z = \frac{-ig}{\cos\theta_W}\Big[\bar{v}(p_1)\gamma^\mu \frac{1}{2}(g_V^e - g_A^e\gamma_5)u(p_2)\Big]\frac{(-g_{\mu\nu} + p_\mu p_\nu/M_Z^2)}{\Big[(p_1+p_2)^2 - M_Z^2 - i\Gamma_Z^2\Big]}\Big[\frac{2M_Z^2\cos\alpha}{v}\Big]\epsilon_\lambda^\nu(Z), \quad (24)$$

$$\begin{aligned}
\mathcal{M}_{Z'} = \quad & \frac{-ig}{\cos\theta_W}\Big[\bar{v}(p_1)\gamma^\mu \frac{1}{2}(g_V'^e - g_A'^e\gamma_5)u(p_2)\Big]\frac{(-g_{\mu\nu} + p_\mu p_\nu/M_{Z'}^2)}{\Big[(p_1+p_2)^2 - M_{Z'}^2 - i\Gamma_{Z'}^2\Big]}\Big[\frac{2M_Z^2}{v}\Big] \\
& \times\Big[f(\theta_{BL}, g_1')\cos\alpha + g(\theta_{BL}, g_1')\sin\alpha\Big]\epsilon_\lambda^\nu(Z), \quad (25)
\end{aligned}$$

where $\epsilon_\lambda^\nu(Z)$ is the polarization vector of the Z boson. The couplings g_V^e, g_A^e, $g_V'^e$, $g_A'^e$ are given in Table II and the functions $f(\theta_{BL}, g_1')$ and $g(\theta_{BL}, g_1')$ are given in Eq. (23), while $\Gamma_{Z'}$ is obtained of Eqs. (18)-(22).

The parameters of the $U(1)_{B-L}$ model, $M_{Z'}$, g'_1, θ_{BL} and α, contribute to the total cross section for the process $e^+e^- \to (Z, Z') \to Zh$, and the expressions for the total cross section of the Higgs-strahlung process for the different contributions can be written in the following compact form [69]:

$$\sigma_{Tot}(e^+e^- \to Zh) = \sigma_Z(e^+e^- \to Zh) + \sigma_{Z'}(e^+e^- \to Zh) + \sigma_{Z,Z'}(e^+e^- \to Zh), \tag{26}$$

where

$$\sigma_Z(e^+e^- \to Zh) = \frac{G_F^2 M_Z^4 \cos^2\alpha}{24\pi}[(g_V^e)^2 + (g_A^e)^2]\frac{s\sqrt{\lambda}[\lambda + 12M_Z^2/s]}{[(s-M_Z^2)^2 + M_Z^2\Gamma_Z^2]}, \tag{27}$$

$$\begin{aligned}\sigma_{Z'}(e^+e^- \to Zh) \;=\; & \frac{G_F^2 M_Z^6}{24\pi}[(g_V^{'e})^2 + (g_A^{'e})^2]\frac{s\sqrt{\lambda}[\lambda + 12M_{Z'}^2/s]}{M_{Z'}^2[(s-M_{Z'}^2)^2 + M_{Z'}^2\Gamma_{Z'}^2]} \\ & \times\; [f(\theta_{BL}, g'_1)\cos\alpha + g(\theta_{BL}, g'_1)\sin\alpha]^2,\end{aligned} \tag{28}$$

$$\begin{aligned}\sigma_{Z,Z'}(e^+e^- \to Zh) \;=\; & \frac{G_F^2 M_Z^6 \cos\alpha}{6\pi}[g_V^e g_V^{'e} + g_A^e g_A^{'e}]s\sqrt{\lambda}\Big[\frac{1}{M_Z^2}(\lambda + 12M_Z^2/s) \\ & +\; \frac{1}{M_{Z'}^2}(\lambda + 6(M_Z^2 - M_{Z'}^2)/s) + \frac{s\lambda}{8M_Z^2M_{Z'}^2}(\lambda - 12M_Z^2/s)\Big] \\ & \times\; \frac{[(s-M_Z^2)(s-M_{Z'}^2) + M_Z M_{Z'}\Gamma_Z\Gamma_{Z'}]}{[(s-M_Z^2)^2 + M_Z^2\Gamma_Z^2][(s-M_{Z'}^2)^2 + M_{Z'}^2\Gamma_{Z'}^2]} \\ & \times\; [f(\theta_{BL}, g'_1)\cos\alpha + g(\theta_{BL}, g'_1)\sin\alpha],\end{aligned} \tag{29}$$

with

$$\lambda\Big(1, \frac{M_Z^2}{s}, \frac{M_h^2}{s}\Big) = \Big(1 - \frac{M_Z^2}{s} - \frac{M_h^2}{s}\Big)^2 - 4\frac{M_Z^2 M_h^2}{s^2}, \tag{30}$$

the usual two-particle phase space function.

The expression given in Eq. (27) corresponds to the cross section with the exchange of the Z boson, while the expressions given in Eqs. (28) and (29) come from the contributions of the B-L model and of the interference, respectively. The SM expression for the cross section of the reaction $e^+e^- \to Zh$ can be obtained in the decoupling limit when $\theta_{BL} = 0$, $g'_1 = 0$ and $\alpha = 0$. In this case, the terms that depend on θ_{BL}, g'_1 and α in Eqs. (27)-(29) are zero and Eq. (26) is reduced to the expression given in Refs. [46, 50] for the standard model.

V. THE DECAY WIDTHS OF THE H HIGGS BOSON IN THE B-L MODEL

In this section we present the decay widths of the H Higgs boson [4, 5, 79] in the context of the B-L model which we need to study the process $e^+e^- \to ZH$. The decay width of the H boson to fermions is given by

$$\Gamma(H \to f\bar{f}) = \frac{G_F M_f^2 M_H}{4\pi\sqrt{2}} N_f \sqrt{\left(1 - \frac{4M_f^2}{M_H^2}\right)^3} \sin^2\alpha, \tag{31}$$

where N_f is the color factor, 1 for leptons and 3 for quarks.

The H partial decay widths involving vector bosons, heavy neutrinos and the scalar boson are

$$\Gamma(H \to W^+W^-) = \frac{G_F M_H^3}{8\pi\sqrt{2}} \sqrt{1 - \frac{4M_W^2}{M_H^2}} \Big[1 - 4\frac{M_W^2}{M_H^2} + \frac{3}{4}\Big(\frac{4M_W^2}{M_H^2}\Big)^2\Big] \sin^2\alpha, \tag{32}$$

$$\Gamma(H \to ZZ) = \frac{G_F M_H^3}{16\pi\sqrt{2}} \sqrt{1 - \frac{4M_Z^2}{M_H^2}} \Big[1 - 4\frac{M_Z^2}{M_H^2} + \frac{3}{4}\Big(\frac{4M_Z^2}{M_H^2}\Big)^2\Big] \sin^2\alpha, \tag{33}$$

$$\Gamma(H \to \nu_R\nu_R) = \frac{M_{\nu_R}^2 M_H}{16\pi v'^2} \sqrt{\left(1 - \frac{4M_{N_R}^2}{M_H^2}\right)^3} \cos^2\alpha, \tag{34}$$

$$\Gamma(H \to hh) = \frac{g_{hhH}^2}{32\pi M_H} \sqrt{1 - \frac{4M_h^2}{M_H^2}}, \tag{35}$$

where the coupling g_{hhH}^2 is given in Table I.

VI. THE HIGGS-STRAHLUNG PROCESS $e^+e^- \to ZH$ IN THE B-L MODEL

In this section, we calculate the Higgs production cross section via the process $e^+e^- \to ZH$ in the context of the $U()_{B-L}$ model at future high-energy and high-luminosity linear electron-positron colliders such as the ILC and CLIC.

The Feynman diagrams contributing to the process $e^+e^- \to (Z, Z') \to ZH$ are shown in Fig. 1. The respective transition amplitudes are thus given by

$$\mathcal{M}_Z = \frac{-ig}{\cos\theta_W}\Big[\bar{v}(p_1)\gamma^\mu \frac{1}{2}(g_V^e - g_A^e\gamma_5)u(p_2)\Big] \frac{(-g_{\mu\nu} + p_\mu p_\nu/M_Z^2)}{\Big[(p_1+p_2)^2 - M_Z^2 - i\Gamma_Z^2\Big]} \Big[\frac{2M_Z^2 \sin\alpha}{v}\Big] \epsilon_\lambda^\nu, \tag{36}$$

$$\mathcal{M}_{Z'} = \frac{-ig}{\cos\theta_W}\Big[\bar{v}(p_1)\gamma^\mu\frac{1}{2}(g_V^{'e} - g_A^{'e}\gamma_5)u(p_2)\Big]\frac{(-g_{\mu\nu} + p_\mu p_\nu/M_{Z'}^2)}{\Big[(p_1+p_2)^2 - M_{Z'}^2 - i\Gamma_{Z'}^2\Big]}[\frac{2M_Z^2}{v}\Big] \times\Big[f(\theta_{BL}, g_1')\sin\alpha - g(\theta_{BL}, g_1')\cos\alpha\Big]\epsilon_\lambda^\nu. \quad (37)$$

Following a similar procedure as that of Section IV, we show our results for the total cross section of the Higgs-strahlung process for the different contributions which can be written in the following compact form:

$$\sigma_{Tot}(e^+e^- \to ZH) = \sigma_Z(e^+e^- \to ZH) + \sigma_{Z'}(e^+e^- \to ZH) + \sigma_{Z,Z'}(e^+e^- \to ZH), \quad (38)$$

where

$$\sigma_Z(e^+e^- \to ZH) = \frac{G_F^2 M_Z^4 \sin^2\alpha}{24\pi}[(g_V^e)^2 + (g_A^e)^2]\frac{s\sqrt{\lambda}[\lambda + 12M_Z^2/s]}{[(s-M_Z^2)^2 + M_Z^2\Gamma_Z^2]}, \quad (39)$$

$$\begin{aligned}\sigma_{Z'}(e^+e^- \to ZH) &= \frac{G_F^2 M_Z^6}{24\pi}[(g_V^{'e})^2 + (g_A^{'e})^2]\frac{s\sqrt{\lambda}[\lambda + 12M_{Z'}^2/s]}{M_{Z'}^2[(s-M_{Z'}^2)^2 + M_{Z'}^2\Gamma_{Z'}^2]} \\ &\times [f(\theta_{BL}, g_1')\sin\alpha - g(\theta_{BL}, g_1')\cos\alpha]^2, \end{aligned} \quad (40)$$

$$\begin{aligned}\sigma_{Z,Z'}(e^+e^- \to ZH) &= \frac{G_F^2 M_Z^6 \sin\alpha}{6\pi}[g_V^e g_V^{'e} + g_A^e g_A^{'e}]s\sqrt{\lambda}\Big[\frac{1}{M_Z^2}(\lambda + 12M_Z^2/s) \\ &+ \frac{1}{M_{Z'}^2}(\lambda + 6(M_Z^2 - M_{Z'}^2)/s) + \frac{s\lambda}{8M_Z^2M_{Z'}^2}(\lambda - 12M_Z^2/s)\Big] \\ &\times \frac{[(s-M_Z^2)(s-M_{Z'}^2) + M_Z M_{Z'}\Gamma_Z\Gamma_{Z'}]}{[(s-M_Z^2)^2 + M_Z^2\Gamma_Z^2][(s-M_{Z'}^2)^2 + M_{Z'}^2\Gamma_{Z'}^2]} \\ &\times [f(\theta_{BL}, g_1')\sin\alpha - g(\theta_{BL}, g_1')\cos\alpha], \end{aligned} \quad (41)$$

with

$$\lambda\Big(1, \frac{M_Z^2}{s}, \frac{M_H^2}{s}\Big) = \Big(1 - \frac{M_Z^2}{s} - \frac{M_H^2}{s}\Big)^2 - 4\frac{M_Z^2 M_H^2}{s^2}. \quad (42)$$

The expression given in Eq. (39) corresponds to the cross section with the exchange of the Z boson, while the expressions given in Eqs. (40) and (41) come from the contributions of the B-L model and of the interference, respectively. In the decoupling limit when $\theta_{BL} = 0$, $g_1' = 0$ and $\alpha = 0$, the total cross section of the reaction $e^+e^- \to ZH$ is zero.

VII. RESULTS AND CONCLUSIONS

A. Higgs boson production and decay h in the B-L model

In this section we evaluate the total cross section of the Higgs-strahlung process $e^+e^- \to (Z, Z') \to Zh$ in the context of the B-L model at next generation linear e^+e^- colliders such as the ILC and CLIC. Using the following values for numerical computation [72]: $\sin^2\theta_W = 0.23126 \pm 0.00022$, $m_\tau = 1776.82 \pm 0.16\, MeV$, $m_b = 4.6 \pm 0.18\, GeV$, $m_t = 172 \pm 0.9\, GeV$, $M_W = 80.389 \pm 0.023\, GeV$, $M_Z = 91.1876 \pm 0.0021\, GeV$, $\Gamma_Z = 2.4952 \pm 0.0023\, GeV$, $M_h = 125 \pm 0.4\, GeV$ and considering the most recent limit from [62, 76, 77]:

$$\frac{M_{Z'}}{g'_1} \geq 6.9\, TeV, \tag{43}$$

it is possible to obtain a direct bound on the B-L breaking scale v' and take $v' = 3.45\, TeV$ and $\alpha = \frac{\pi}{9}$. In our numerical analysis, we obtain the total cross section $\sigma_{tot} = \sigma_{tot}(\sqrt{s}, M_{Z'}, g'_1, \theta_{BL}, \alpha)$. Thus, in our numerical computation, we will assume $\sqrt{s}$, $M_{Z'}$, g'_1, θ_{BL} and α as free parameters.

In order to determine how $g_{ZZ'h}$ coupling change from their SM value, as well as the functions $f(\theta_{BL}, g'_1)$ and $g(\theta_{BL}, g'_1)$ with respect to the parameters of the B-L model, we give a 2D plot in Fig. 2. As seen from this figure, both the $g_{ZZ'h}$ coupling and the functions $f(\theta_{BL}, g'_1)$ and $f(\theta_{BL}, g'_1)$ strongly depend on g'_1.

In Fig. 3 we present the total decay width of the Z' boson as a function of $M_{Z'}$ and the new $U(1)_{B-L}$ gauge coupling g'_1, respectively, with the other parameters held fixed to three different values. From the top panel, we see that the total width of the Z' new gauge boson varies from very few to hundreds of GeV over a mass range of $1000\, GeV \leq M_{Z'} \leq 3500\, GeV$, depending on the value of g'_1, when $g'_1 = 0.145, 0.290, 0.435$, respectively. In the case of the bottom panel, a similar behavior is obtained in the range $0 \leq g'_1 \leq 1$ and depends on the value $M_{Z'} = 1000, 2000, 3000\, GeV$. The branching ratios versus Z' mass and the coupling g'_1 are given in Fig. 4 for different channels: $BR(Z' \to f\bar{f})$, $BR(Z' \to W^+W^-)$, $BR(Z' \to Zh)$, $BR(Z' \to ZH)$ and $BR(Z' \to \nu_R\bar{\nu}_R)$, respectively. In these figures, the $BR(Z' \to f\bar{f})$ is the sum of all BRs for the decays into fermions. In the case of the top panel, we consider $\theta_{B-L} = 10^{-3}$, $g'_1 = 0.290$ and $1000\, GeV \leq M_{Z'} \leq 3500\, GeV$. For the bottom panel, we consider $\theta_{B-L} = 10^{-3}$, $M_{Z'} = 2000\, GeV$ and $0 \leq g'_1 \leq 1$. In both figures a clear dependence

is observed on the parameters of the $U(1)_{B-L}$ model.

We present Figs. 5-9 to illustrate our results regarding the sensitivity of the Z' heavy gauge boson of the B-L model as a Higgs boson source through the Higgs-strahlung process $e^+e^- \to (Z, Z') \to Zh$, including both the resonant and non-resonant effects at future high-energy and high luminosity linear e^+e^- colliders, such as the ILC and the CLIC.

In Fig. 5, we show the cross section $\sigma(e^+e^- \to Zh)$ for the different contributions as a function of the center-of-mass energy $\sqrt{s}$ for $\theta_{B-L} = 10^{-3}$ and $g_1' = 0.290$: the solid line corresponds to the SM and the dashed line corresponds to $\sigma_Z(e^+e^- \to Zh)$ (Eq. (27)), where the $U(1)_{B-L}$ model contributes to the couplings g_V^f and g_A^f of the SM gauge boson Z to electrons. The dot-dashed line corresponds to $\sigma_{Z'}(e^+e^- \to Zh)$ (Eq. (28)), which is only the B-L contribution, while the dot dot-dashed line corresponds to the interference $\sigma_{Z,Z'}(e^+e^- \to Zh)$ (Eq. (29)). Finally, the dot line corresponds to the total cross section of the process $e^+e^- \to Zh$ (Eq. (26)). In Figure 5, we can see that the cross section corresponding to $\sigma_Z(e^+e^- \to Zh)$ decreases for large $\sqrt{s}$, whereas in the case of the cross section of the B-L model Eq. (28) and the total cross section Eq. (26), respectively, there is an increased for large values of the center-of-mass energy, reaching its maximum value at the resonance Z' heavy gauge boson, which is to say, $\sqrt{s} = 2000\, GeV$.

We plot the total cross section of the reaction $e^+e^- \to Zh$ in Fig. 6 as a function of the center-of-mass energy, $\sqrt{s}$ for the values of the heavy gauge boson mass of $M_{Z'} = 1000, 2000, 3000\, GeV$ and $g_1' = 0.145, 0.290, 0.435$, respectively. It is worth mentioning that the choice of the values for $M_{Z'}$ and g_1' is accomplished by maintaining the relationship between $M_{Z'}$ and g_1' given by Eq. (43). This relationship will always remain throughout the article. In Fig. 6 we show that the cross section is sensitive to the free parameters and also observe that the height of the resonance peaks for the boson Z' changes depending on the value of $\sqrt{s} = M_{Z'}^2$. In addition, the resonances are broader for larger g_1' values, as the total width of the Z' boson increases with g_1', as shown in Fig. 3.

An important quantity is the statistical significance,

$$S[\sigma] = \frac{|\sigma_{Zh}^{BL} - \sigma_{Zh}^{SM}|}{\delta\sigma_{Zh}^{BL}} = \frac{|\Delta\sigma_{Zh}|}{\sqrt{\sigma_{Zh}^{SM}}}\sqrt{\mathcal{L}_{int}}, \tag{44}$$

where $\delta\sigma_{Zh}$ is the statistical uncertainty, and $\mathcal{L}$ the integrated luminosity. It determines the deviation of the cross section from the SM prediction, in terms of standard deviations. In

Fig. 7 we show the energy dependence of this statistical significance for $\mathcal{L} = 1000\, fb^{-1}$, and for three different masses, $M_{Z'}$ with its corresponding value for g_1': $M_{Z'} = 1000\, GeV$ and $g_1' = 0.145$, $M_{Z'} = 2000\, GeV$ and $g_1' = 0.290$, $M_{Z'} = 3000\, GeV$ and $g_1' = 0.435$, respectively. As seen in the figure, the peaks are located at energies of $\sqrt{s} = 1000, 2000, 3000\, GeV$. The figure also shows that the sensitivity is reduced at higher Z' masses. The statistical significance $S[\sigma]$ as a function of g_1' is shown in Fig. 8 for $M_{Z'} = 1000, 2000, 3000\, GeV$ and $\sqrt{s} = 1000, 2000, 3000\, GeV$ with $\mathcal{L} = 1000\, fb^{-1}$, respectively. It is clear that the $S[\sigma]$ increases as g_1' increases, and demonstrates a clear dependence on the parameters of the model. Thus, in a sizeable parameter region of the B-L model, the new heavy gauge boson Z' can produce a significant signal which can be detected in future ILC and CLIC experiments.

The correlation between the heavy gauge boson mass $M_{Z'}$ and the g_1' coupling of the $U(1)_{BL}$ model for the cross section of $\sigma_{Tot} = 100, 200, 400, 500\, fb$ (top panel) with $\sqrt{s} = 1000\, GeV$, $\sigma_{Tot} = 10, 20, 30, 35\, fb$ (central panel) with $\sqrt{s} = 2000\, GeV$ and $\sigma_{Tot} = 4, 5, 6, 7\, fb$ (bottom panel) with $\sqrt{s} = 3000\, GeV$ is presented in Fig. 9. From the plots we see that there is a strong correlation between the gauge boson mass $M_{Z'}$ and the new gauge coupling g_1'.

TABLE III: Total production of Zh in the B-L model for $M_{Z'} = 1000, 2000, 3000\, GeV$, $\mathcal{L} = 500, 1500, 2000\ fb^{-1}$, $M_h = 125\, GeV$, $\alpha = \pi/9$ and $\theta_{B-L} = 10^{-3}$.

$\mathcal{L} = 500; 1500; 2000\ fb^{-1}$			
$\sqrt{s}\ (GeV)$	$M_{Z'} = 1000\, GeV$ $g_1' = 0.145$	$M_{Z'} = 2000\, GeV$ $g_1' = 0.290$	$M_{Z'} = 3000\, GeV$ $g_1' = 0.435$
1000	227280; 681841; 909124		
2000		16502; 49506; 66008	
3000			3788; 11365; 15154

From Figs. 5-9, it is clear that the total cross section is sensitive to the value of the gauge boson mass $M_{Z'}$, center-of-mass energy $\sqrt{s}$ and g_1', which is the new $U(1)_{B-L}$ gauge coupling. The total cross section increases with the collider energy and reaching a maximum at the resonance of the Z' gauge boson. As an indicator of the order of magnitude, we

present the Zh number of events in Table III for several center-of-mass energies $\sqrt{s} = 1000, 2000, 3000\, GeV$, integrated luminosity $\mathcal{L} = 500, 1500, 2000\, fb^{-1}$ and heavy gauge boson masses $M_{Z'} = 1000, 2000, 3000\, GeV$ with $g_1' = 0.145, 0.290, 0.435$, respectively. It is worth mentioning that the values reported in Table III for the total number of events Zh are determined while preserving the relationship between $M_{Z'}$ and g_1' given in Eq. (43). We find that the possibility of observing the process $e^+e^- \to (Z, Z') \to Zh$ is very promising as shown in Table III, and it would be possible to perform precision measurements for both the Z' and Higgs boson in the future high-energy and high-luminosity linear e^+e^- colliders experiments. We observe in Table III that the cross section rises once the threshold for Zh production is reached, with the energy, until the Z' is produced resonantly at $\sqrt{s} = 1000, 2000$ and 3000 GeV, respectively, for the three cases. Afterwards it decreases with rising energy due to the Z and Z' propagators. Another promising production mode for studying the Z' boson and Higgs boson properties of the B-L model is $e^+e^- \to (Z, Z') \to ZH$, which is studied in the next subsection.

B. Heavy Higgs boson production and decay H in the B-L model

As in the previous subsection, in this study we use the Higgs-strahlung process $e^+e^- \to (Z, Z') \to ZH$ to investigate the impact of the parameters of the B-L model on this process. First, we present Fig. 10 in order to analyze the behavior of the coupling $g_{ZZ'H}$, as well as of the functions $f(\theta_{BL}, g_1')$ and $g(\theta_{BL}, g_1')$ with respect to the parameters of the model. From this figure is clear that both the coupling $g_{ZZ'H}$ and the functions $f(\theta_{BL}, g_1')$ and $g(\theta_{BL}, g_1')$ are sensitive to the parameters of the model.

In Fig. 11, we present the total decay width of the H heavy Higgs boson as a function of M_H and on the scalar mixing $cos\alpha$, respectively. In the top panel figure, we observed that total width of the H Higgs boson varies from a few to hundreds of GeV over a mass range of $400\, GeV \leq M_H \leq 1000\, GeV$, depending on the value de $cos\alpha$, i.e. $cos\alpha = 0.2, 0.4, 0.6, 0.8$, respectively. In the bottom panel figure, we show the dependence of total decay width of the heavy scalar boson Γ_H on the scalar mixing $cos\alpha$ for different values of M_H and a moderate value of the mass of the heavy neutrinos $M_{\nu_R} = 300\, GeV$. For higher M_H, the decay width becomes larger for large mixing. This plot also shows that for the limiting case when $\cos\alpha \to 1$, without mixing between the scalar bosons, $\Gamma_{Tot}(H) \to 0$ and hence it is

completely decoupled from the SM.

In Fig. 12, the top panel shows the branching fractions of H decays in $f\bar{f}$, W^-W^+, ZZ, hh and $\nu_R\bar{\nu}_R$ as function of its mass, varying M_H between $400\,GeV$ and $1000\,GeV$ for $M_{\nu_R} = 300\,GeV$ and $\alpha = \frac{\pi}{6}$. As is clear from top panel, the three most dominant decay modes of H are W^-W^+, ZZ and $f\bar{f}$. The bottom panel shows the branching ratios of H as function of the scalar mixing $cos\alpha$ for a given value of $M_H = 800\,GeV$ and $M_{\nu_R} = 300\,GeV$. The W^-W^+ pairs clearly dominate the H decays.

The total cross section for the Higgs-strahlung production processes $e^+e^- \to ZH$ as a function of the collision energy for $M_h = 125\,GeV$, $M_H = 800\,GeV$, $M_{\nu_R} = 300\,GeV$, $M_{Z'} = 2000\,GeV$ and $g'_1 = 0.290\,GeV$ is shown in Fig. 13. In this figure the curves are for $\sigma_Z(e^+e^- \to ZH)$ (Eq. (39)) (solid line), $\sigma_{Z'}(e^+e^- \to ZH)$ (Eq. (40)) (dashed line), $\sigma_{Z,Z'}(e^+e^- \to ZH)$ (Eq. (41)) (dot-dashed line), and the dot dot-dashed line corresponds to the total cross section of the process $\sigma_{Tot}(e^+e \to ZH)$ (Eq. (38)), respectively.

To see the effects of θ_{BL}, g'_1, $M_{Z'}$, the free parameters of the B-L model, we plot the total cross section of the process $e^+e^- \to ZH$ in Fig. 14 as a function of the center-of-mass energy $\sqrt{s}$ for the values of the heavy gauge boson mass of $M_{Z'} = 1000\,GeV$ with $g'_1 = 0.145$, $M_{Z'} = 2000\,GeV$ with $g'_1 = 0.290$ and $M_{Z'} = 3000\,GeV$ with $g'_1 = 0.435$, respectively, preserving the relationship between $M_{Z'}$ and g'_1 given by Eq. (43). In this figure we observed that for $\sqrt{s} = M_{Z'}$, the resonant effect dominates, the cross section is sensitive to the free parameters. We also observe that the height of the resonance peaks for the boson Z' change depending on the value of $\sqrt{s} = M^2_{Z'}$, and in addition, that the resonances are broader for larger g'_1 values, as the total width of the Z' boson increases with g'_1, as is shown in Fig. 3.

In Fig. 15, we show the correlation between the heavy gauge boson mass $M_{Z'}$ and the g'_1 coupling of the $U(1)_{BL}$ model for the cross section of $\sigma_{Tot} = 10, 20, 30, 40\,fb$ (top panel), $\sigma_{Tot} = 1, 1.5, 2, 3\,fb$ (central panel) and $\sigma_{Top} = 0.3, 0.4, 0.5, 0.7\,fb$ (bottom panel). From the plots we see that there is a strong correlation between $M_{Z'}$ and g'_1.

Finally, from Figs. 13-15, it is clear that the total cross section is sensitive to the value of the gauge boson mass $M_{Z'}$, center-of-mass energy $\sqrt{s}$ and g'_1, which is, the new $U(1)_{B-L}$ gauge coupling, increases with the collider energy and reaching a maximum at the resonance of the Z' gauge boson. As an indicator of the order of magnitude, we present the ZH number of events in Table IV, for several center-of-mass energies

TABLE IV: Total production of ZH in the B-L model for $M_{Z'} = 1000, 2000, 3000\, GeV$, $\mathcal{L} = 500, 1500, 2000\ fb^{-1}$, $M_H = 800\, GeV$, $\alpha = \pi/9$ and $\theta_{B-L} = 10^{-3}$.

$\mathcal{L} = 500; 1500; 2000\ fb^{-1}$			
$\sqrt{s}\ (GeV)$	$M_{Z'} = 1000\, GeV$ $g_1' = 0.145$	$M_{Z'} = 2000\, GeV$ $g_1' = 0.290$	$M_{Z'} = 3000\, GeV$ $g_1' = 0.435$
1000	24371; 73115; 97487		
2000		1437; 4312; 5750	
3000			289; 869; 1158

$\sqrt{s} = 1000, 2000, 3000\, GeV$, integrated luminosity $\mathcal{L} = 500, 1500, 2000\ fb^{-1}$ and heavy gauge boson masses $M_{Z'} = 1000, 2000, 3000\, GeV$ with $g_1' = 0.145, 0.290, 0.435$, respectively. It is worth mentioning that the values reported in Table IV for the total number of events ZH are determined while preserving the relationship between $M_{Z'}$ and g_1' given by Eq. (43). We find that the possibility of observing the process $e^+e^- \to (Z, Z') \to ZH$ is very promising as shown in Table IV, and it would be possible to perform precision measurements for both the Z' and Higgs boson in the future high-energy linear e^+e^- colliders experiments. We observed in Table IV that the cross section rises once the threshold for ZH production is reached, with the energy, until the Z' is produced resonantly at $\sqrt{s} = 1000, 2000$ and 3000 GeV, respectively, for the three cases. Afterwards it decreases with rising energy due to the Z and Z' propagators.

In conclusion, in this article we have studied the phenomenology of the light and heavy Higgs boson production and decay in the context of a $U(1)_{B-L}$ extension of the SM with an additional Z' boson at future e^+e^- linear colliders with center-of-mass energies of $\sqrt{s} = 500 - 3000\, GeV$ and integrated luminosities of $\mathcal{L} = 500 - 2000\ fb^{-1}$. Our study covers the Higgs-strahlung processes $e^+e^- \to (Z, Z') \to Zh$ and $e^+e^- \to (Z, Z') \to ZH$, including both the resonant and non-resonant effects. We find that the total number of expected Zh and ZH events can reach 909,124 and 97,487, respectively, which is a very optimistic scenario and it would be possible to perform precision measurements for both Higgs bosons h and H, for the Z' heavy gauge boson, as well as for the parameters of the model θ_{B-L}, g_1' and α in future high-energy and high-luminosity e^+e^- colliders experiments such as the ILC and

CLIC. In addition, the SM expression for the cross section of the reaction $e^+e^- \to Zh$ can be obtained in the decoupling limit when $\theta_{B-L} = 0$, $g_1' = 0$ and $\alpha = 0$. In this case, the terms that depend on θ_{B-L}, g_1' and α in (26) are zero and (26) is reduced to the expression given in Refs. [46, 50] for the SM. Our study complements other studies on the B-L model and on the Higgs-strahlung processes $e^+e^- \to (Z, Z') \to Zh$ and $e^+e^- \to (Z, Z') \to ZH$.

Acknowledgments

We acknowledge support from CONACyT, SNI and PROFOCIE (México).

[1] W. Buchmuller, C. Greub, and P. Minkowski, *Phys. Lett.* **B267**, 395 (1991).

[2] R. Marshak and R. N. Mohapatra, *Phys. Lett.* **B91**, 222 (1980).

[3] R. N. Mohapatra and R. Marshak, *Phys. Rev. Lett.* **44**, 1316 (1980).

[4] S. Khalil, *J. Phys. G: Nucl. Part. Phys.* **G35**, 055001 (2008).

[5] S. Khalil, *Eur. Phys. J.* **C52**, 625 (2007).

[6] E. D. Carlson, *Nucl. Phys.* **B286**, 378 (1987).

[7] R.N. Mohapatra and G. Senjanovic, *Phys. Rev. Lett.* **44**, 912 (1980).

[8] P. Minkowski, *Phys. Lett.* **B67**, 421 (1977).

[9] P. Van Nieuwenhuizen and D. Z. Freedman, 341 (1979), Amsterdam, Netherlands: North-Holland.

[10] T. Yanagida, in Proceedings of the Workshop on the *Baryon Number of the Universe and Unified Theories*, Tsukuba, Japan, 13-14 February, (1979), p. 95.

[11] M. Gell-Mann, P. Ramond, and R. Slansky print-80-0576 (CERN).

[12] M. Fukugita and T. Yanagida, *Physics of Neutrinos and Applications to Astrophysics*, (Springer, Berlin, 2003).

[13] G. Aad, *et al.,* [ATLAS Collaboration], *Phys. Lett.* **B716**, 1 (2012).

[14] S. Chatrchyan, *et al.,* [CMS Collaboration], *Phys. Lett.* **B716**, 30 (2012).

[15] T. Abe, *et al.* [Am. LC Group], arXiv: hep-ex/0106057.

[16] G. Aarons *et al.,* [ILC Collaboration], arXiv: 0709.1893 [hep-ph].

[17] J. Brau, *et al.,* [ILC Collaboration], arXiv: 0712.1950 [physics.acc-ph].

[18] H. Baer, T. Barklow, K. Fujii, *et al., The International Linear Collider, Technical Desing Report-Vol. 2: Physics*, arXiv:1306.6352 [hep-ph].

[19] D. M. Asner, *et al., ILC Higgs White Paper*, arXiv: 1310.0763 [hep-ph].

[20] *Proceedings of the Workshop e^+e^- Collisions at 500 GeV: The Physics Potential*, Munich-Annecy-Hamburg, ed. P. M. Zerwas, Reports DESY 92-123A, B; 93-123C.

[21] E. Accomando, *et al.* [CLIC Physisc Working Group Collaboration], arXiv: hep-ph/0412251, CERN-2004-005.

[22] H. Abramowicz, *et al.*, *The CLIC Detector and Physics Study*, arXiv:1307.5288 [hep-ex].

[23] D. Dannheim, P. Lebrun, L. Linssen et al., arXiv: 1208.1402 [hep-ex].

[24] L. Basso, *et al., Phys. Rev.* **D80**, 055030 (2009).

[25] L. Basso, *et al., JHEP* **0910**, 006 (2009).

[26] P. Langacker, *Rev. Mod. Phys.* **81**, 1199 (2009).

[27] G. Aad, *et al.*, [ATLAS Collaboration], *Phys. Rev.* **D90**, 052005 (2014).

[28] ATLAS collaboration, ATLAS-CONF-2015-070.

[29] CMS Collaboration, CMS-PAS-EXO-12-023.

[30] V. Khachatryan, *et al.*, [CMS Collaboration], *JHEP* **1504**, 025 (2015).

[31] V. Khachatryan, *et al.*, [CMS Collaboration], *Phys. Rev.* **D91**, 052009 (2015).

[32] S. Chatrchyan, *et al.*, [CMS Collaboration], *JHEP* **1209**, 029 (2012).

[33] G. Aad, *et al.*, [ATLAS Collaboration], [arXiv:1502.07177].

[34] ATLAS Collaboration, ATLAS-CONF-2013-017.

[35] CMS Collaboration, CMS-PAS-EXO-12-061.

[36] CMS Collaboration Collaboration, CMS PAS HIG-13-032.

[37] G. Aad, *et al.*, [ATLAS Collaboration], *Phys. Rev. Lett.* **114**, 081802 (2015).

[38] G. Aad, *et al.*, [ATLAS Collaboration], arXiv:1506.00285.

[39] B. C. Allanach, *et al.,* arXiv:hep-ph/0403133.

[40] L. Basso, *et al., Eur. Phys. J.* **C71**, 1613 (2011).

[41] L. Basso, S. Moretti and G. M. Pruna, *J. Phys. G: Nucl. Part. Phys.* **G39**, 025004 (2012).

[42] L. Basso, S. Moretti and G. M. Pruna, *Phys. Rev.* **D82**, 055018 (2010).

[43] L. Basso, *et al., Eur. Phys. J.* **C71**, 1724 (2011).

[44] L. Basso, arXiv:1106.4462 [hep-hp].

[45] Satoshi Iso, Nobuchica Ocada and Yuta Orikasa, *Phys. Rev.* **D80**, 115007 (2009).

[46] J. Ellis, M. K. Gaillard, and D. V. Nanopoulos, *Nucl. Phys.* **B106**, 292 (1976).

[47] B. L. Ioffe and V. A. Khoze, *Sov. J. Part. Nucl.* **9**, 50 (1978).

[48] B. W. Lee, C. Quigg, and H. B. Thacker, *Phys. Rev.* **D16**, 1519 (1977).

[49] J. D. Bjorken, Proceeding *Summer Institute on Particle Physics*, SLAC Report 198 (1976).

[50] V. D. Barger, *et al., Phys. Rev.* **D49**, 79 (1994).

[51] John Ellis, arXiv:1312.5672.

[52] S. Dawson, *et al.,* [Higgs working group], arXiv:1310.8361.

[53] M. Klute, *et al.,* arXiv:1301.1322.

[54] T. Behnke, *et al.,* arXiv:1306.6327.

[55] G. Weiglein, *et al., The LHC/LC Study Group*, arXiv:hep-ph/0410364.

[56] Abdelhak Djouadi, *Phys. Rept.* **457**, 1 (2008).

[57] M. Gell-Mann, P. Ramond, and R. Slansky, in *Supergravity*, Proceedings of Workshop, Stony Brook, New York, 1979, edited by P. Van Nieuwenhuizen and D. Z. Freedman (North-Holland, Amsterdam, 1979), p 315.

[58] R. E. Marshak and R. N. Mohapatra, *Phys. Lett.* **B91**, 222 (1980).

[59] A. Ferroglia, A. Lorca and J. J. van der Bij, *Ann. Phys.* **16**, 563 (2007); and references therein.

[60] T. G. Rizzo, arXiv:hep-ph/0610104; and references therein.

[61] T. Appelquist, B. A. Dobrescu, and A. R. Hopper, *Phys. Rev.* **D68**, 035012, (2003).

[62] M. Carena, A. Daleo, B. A. Dobrescu, and T. M. Tait, *Phys. Rev.* **D70**, 093009 (2004).

[63] G. Aad, *et al.* [ATLAS Collaboration], *Phys. Lett.* **B726**, 88 (2013).

[64] S. Chatrchyan, *et al. JHEP* **1306**, 081 (2013).

[65] P. Bandyopadhyay, E. J. Chun, H. Okada and J. C. Park, *JHEP* **1301**, 079 (2013).

[66] L. Basso, *Phys. Lett.* **B725**, 322 (2013).

[67] H. Mansour, N. Bakhet, *J. Open Microphys.* **4**, 37 (2013).

[68] S. Schael, *et al.*, *Phys. Rept.* **427**, 257 (2006).

[69] A, Gutiérrez-Rodríguez and M. A. Herández-Ruíz, *Advances in High Energy Physics* **2015**, 593898 (2015).

[70] A, Gutiérrez-Rodríguez, Proceedings *20th International Conference on Particles and Nuclei*

(PANIC 14), Hamburg, Germany; Alexander Schmidt (ed.), Christian Sander (ed.). Conference: C14-08-24, DESY-PROC-2014-04, p. 683.

[71] Shi-Yu, *et al.*, *Int. J. Theor. Phys.* **55**, 648 (2016).

[72] K. A. Olive, *et al.*, [Particle Data Group], *Chin. Phys.* **C38**, 090001 (2014).

[73] A. Leike, *Phys. Rep.* **317**, 143 (1999).

[74] R. W. Robinett and J. L. Rosner, *Phys. Rev.* **D25**, 3036 (1982).

[75] V. Barger and K. Whisnant, *Phys. Rev.* **D36**, 3429 (1987).

[76] J. Heeck, *Phys. Lett.* **B739**, 256 (2014).

[77] G. Cacciapaglia, C. Csaki, G. Marandella and A. Strumia, *Phys. Rev.* **D74**, 033011 (2006).

[78] Lorenzo Basso, Stefano Moretti, and Giovanni Marco Pruna, *Phys. Rev.* **D83**, 055014 (2011).

[79] Tanushree Basak, Tanmoy Mondal, *Phys. Rev.* **D89**, 063527 (2014).

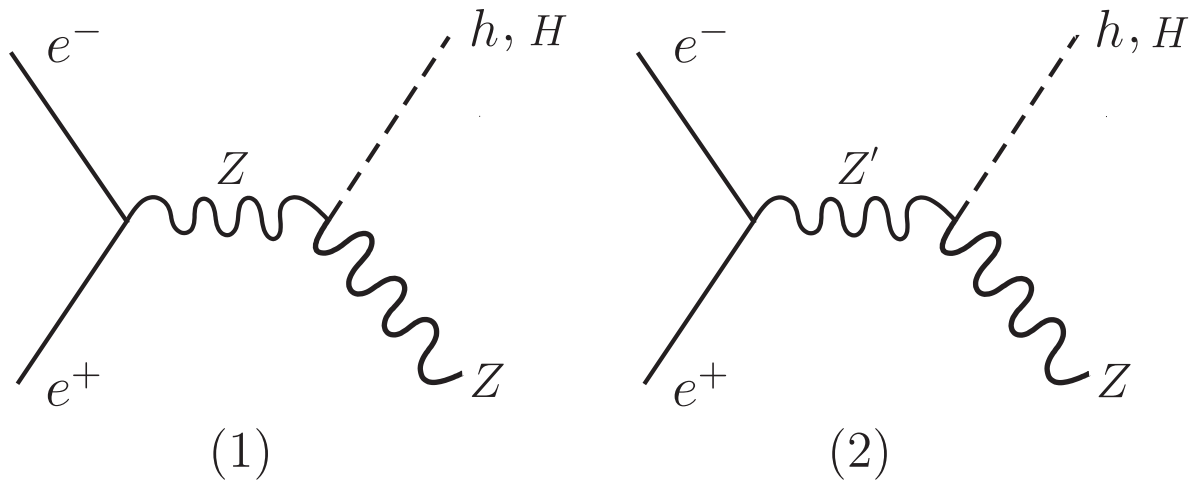

FIG. 1: Feynman diagram for the Higgs-strahlung processes $e^+e^- \to Zh$ and $e^+e^- \to ZH$ in the B-L model.

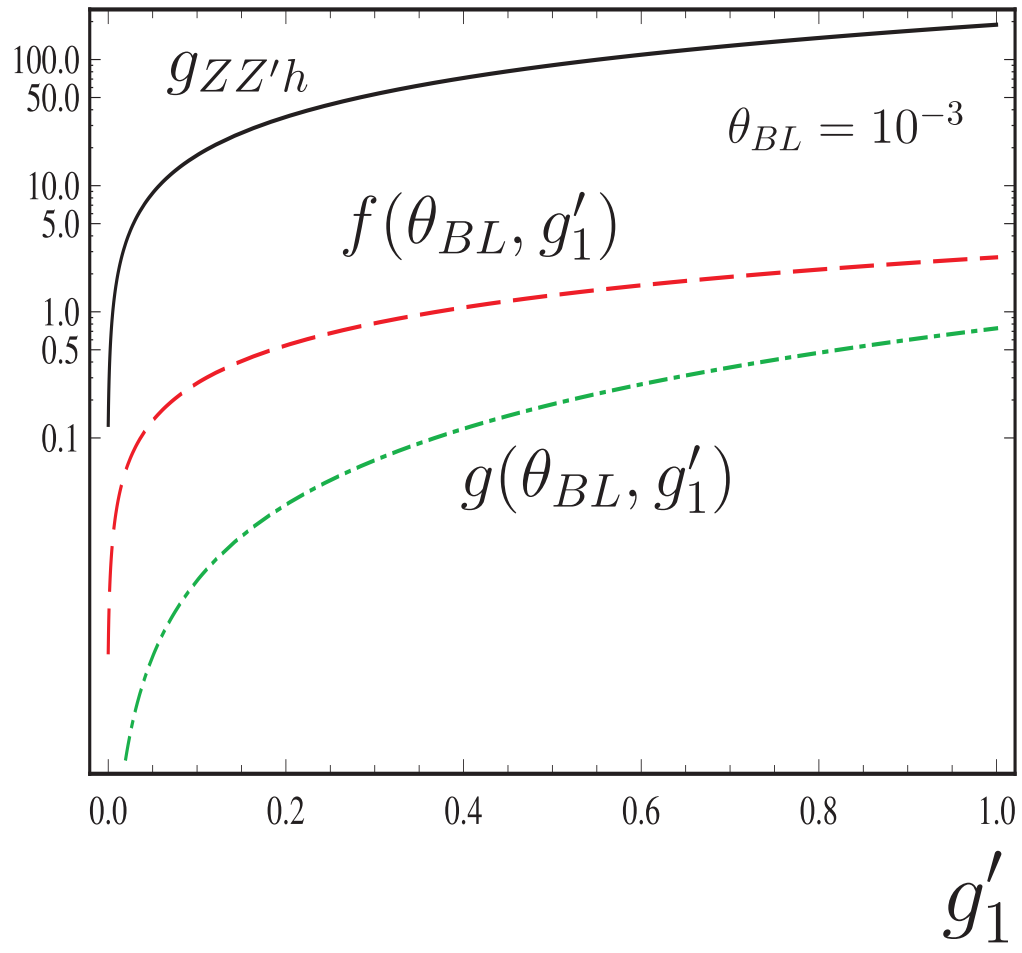

FIG. 2: $g_{ZZ'h}(\theta_{BL}, g_1')$ coupling and $f(\theta_{BL}, g_1')$, $g(\theta_{BL}, g_1')$ functions as a function of g_1', with $\theta_{BL} = 10^{-3}$.

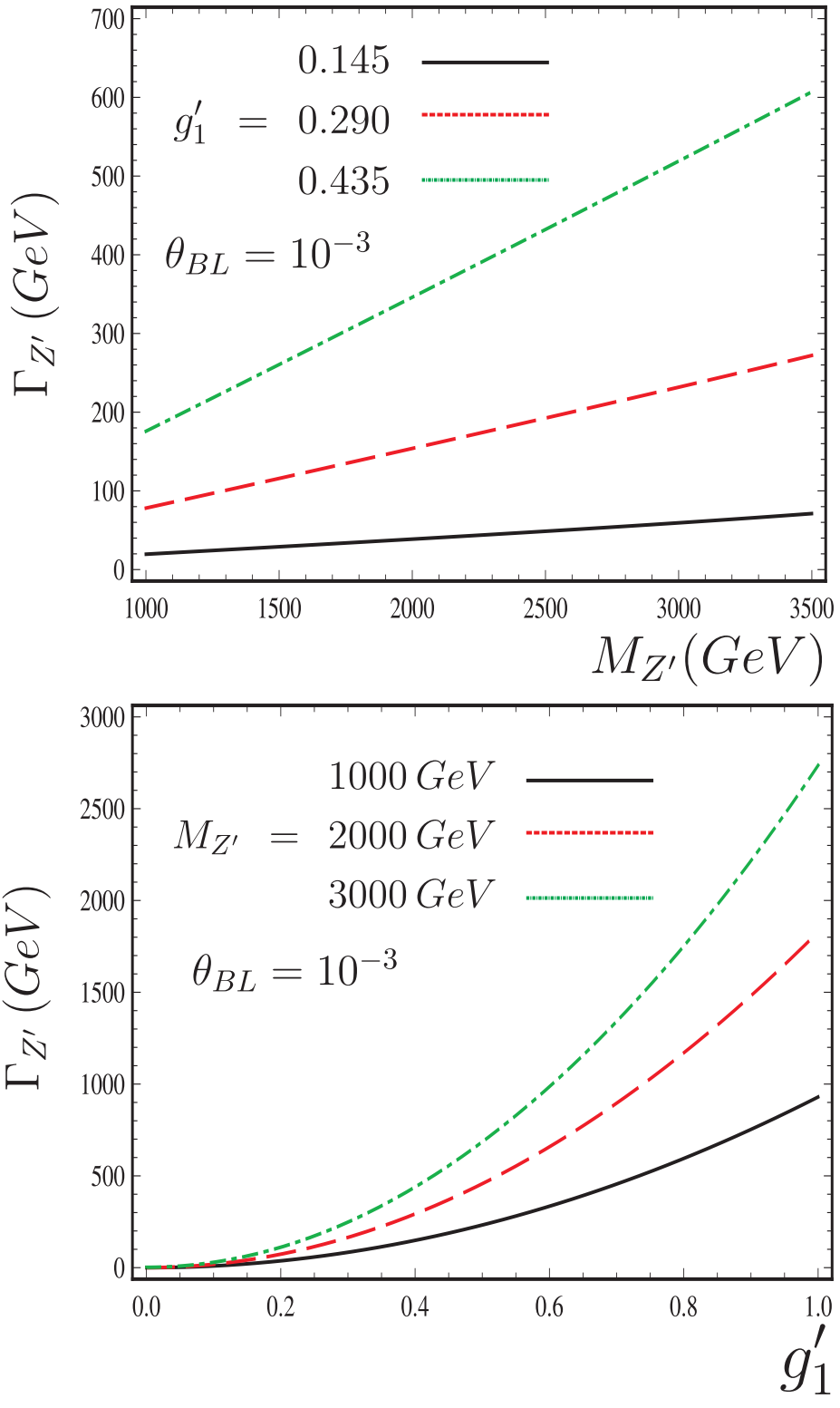

FIG. 3: Top panel: Z' width as a function of $M_{Z'}$ for fixed values of g_1'. Bottom panel: Z' width as a function of g_1' for fixed values of $M_{Z'}$.

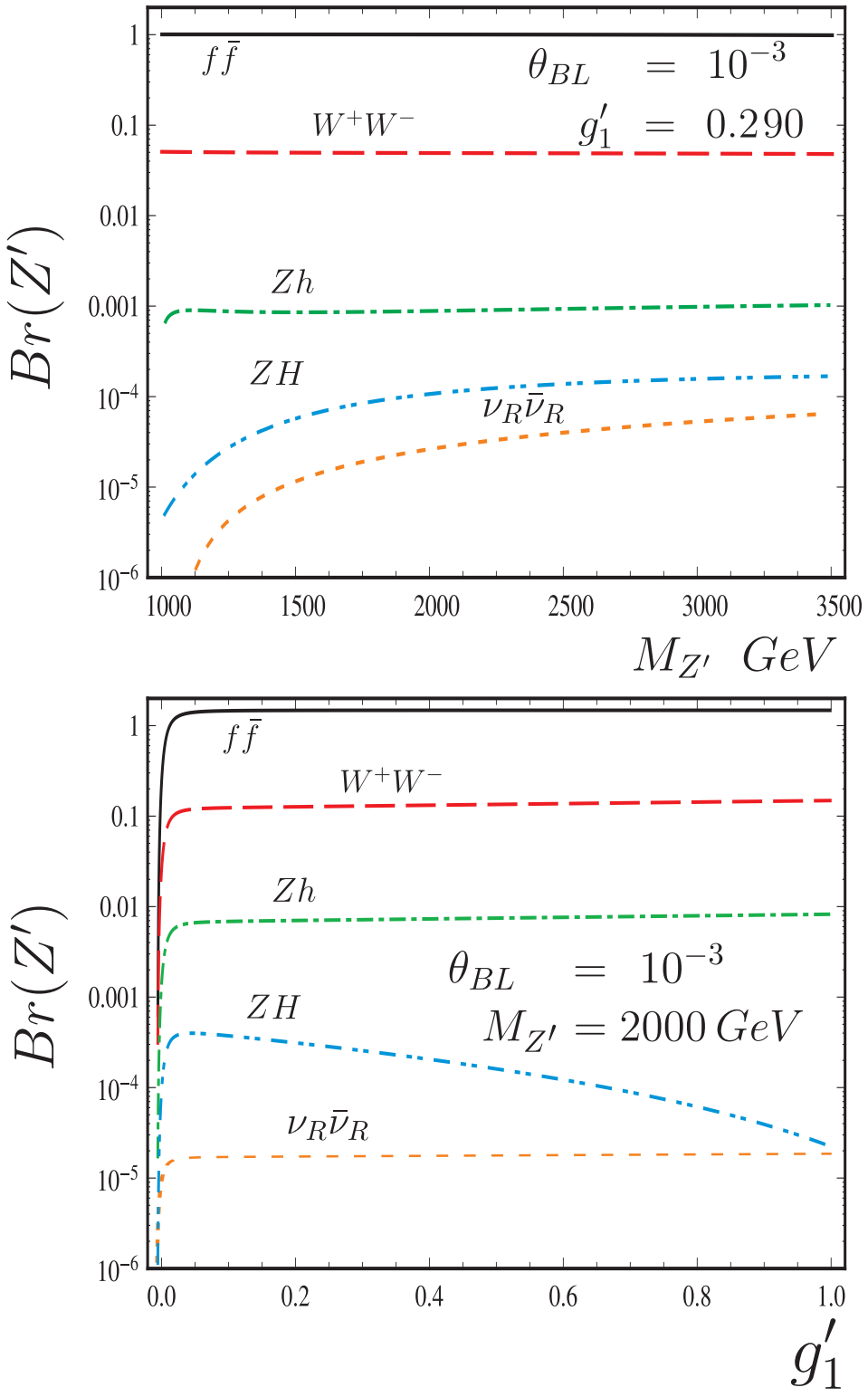

FIG. 4: Top panel: Branching ratios as a function of $M_{Z'}$. Bottom panel: Branching ratios as a function of g_1'.

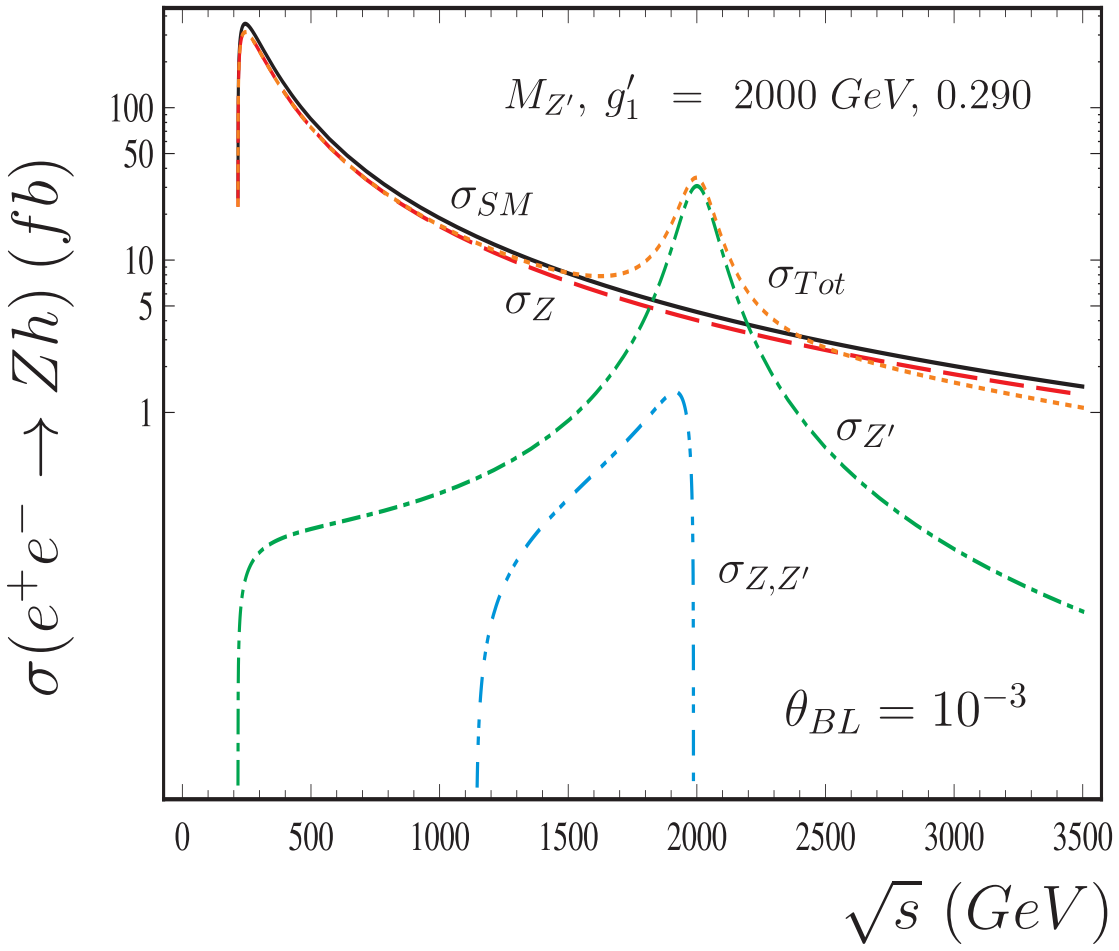

FIG. 5: The cross section of the production process $e^+e^- \to Zh$ as a function of $\sqrt{s}$ for $M_h = 125$ GeV, $M_{Z'} = 2000\,GeV$ and $g_1' = 0.290$. The curves are for the SM (solid line), σ_Z (Eq. (25)) (dashed line), $\sigma_{Z'}$ (Eq. (26)) (dot-dashed line), $\sigma_{Z,Z'}$ (Eq. (27)) (dot dot-dashed line), and the doted line correspond to the total cross section of the process σ_{Tot} (Eq. (24)), respectively.

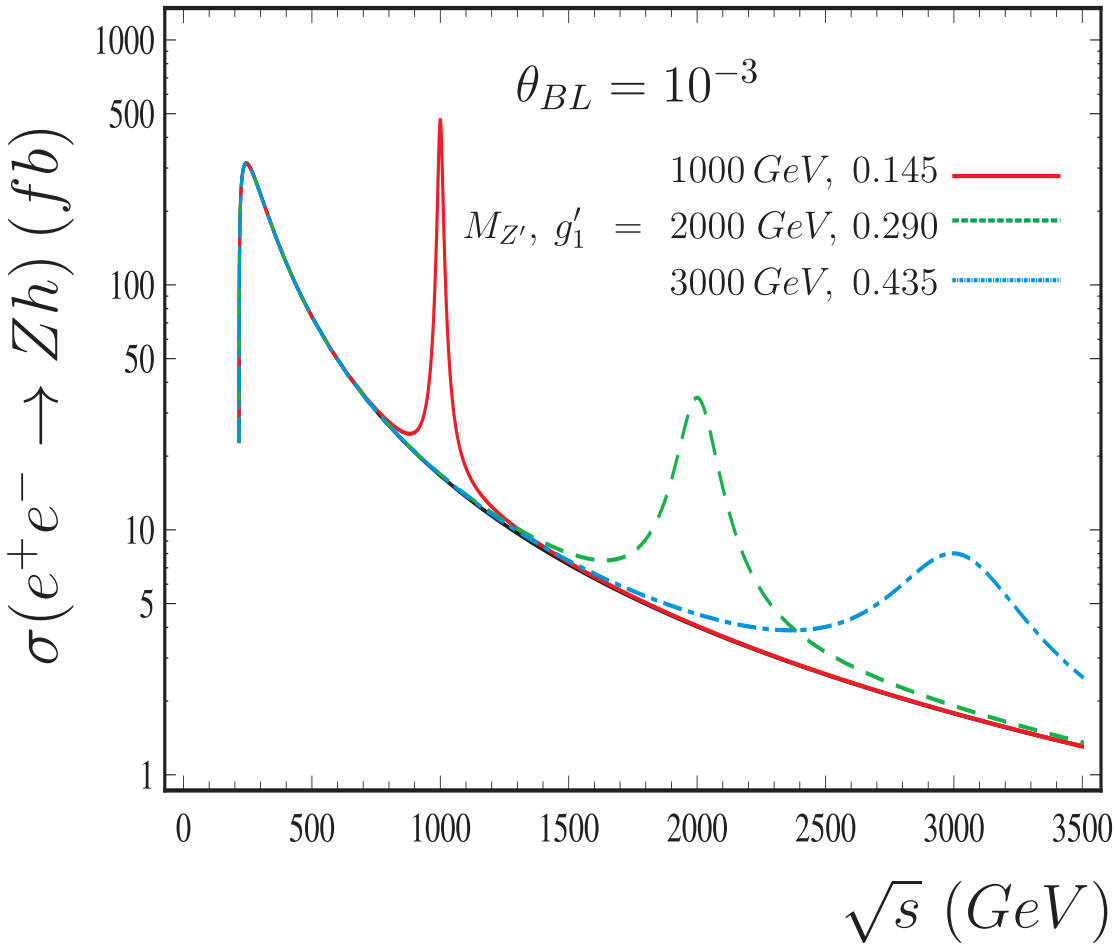

FIG. 6: The total cross section of the production process $e^+e^- \to Zh$ as a function of $\sqrt{s}$. The curves are for $M_{Z'} = 1000\,GeV$ and $g_1' = 0.145$ (solid line), $M_{Z'} = 2000\,GeV$ and $g_1' = 0.290$ (dashed line), $M_{Z'} = 3000\,GeV$ and $g_1' = 0.435$ (dot-dashed line), respectively.

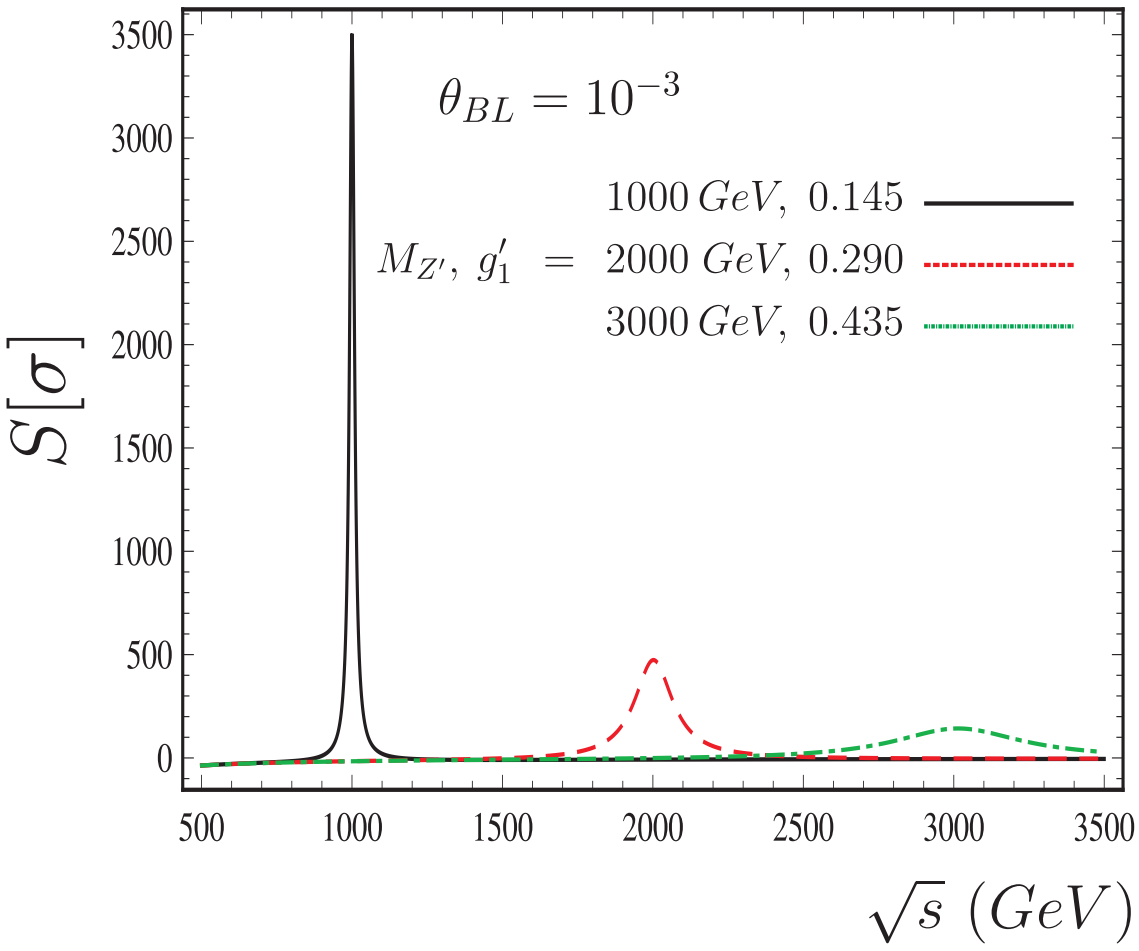

FIG. 7: The statistical significance $S[\sigma]$ of Eq. (41) as a function of $\sqrt{s}$. Starting from the top, the curves are for $M_{Z'} = 1000\,GeV$ and $g_1' = 0.145$, $M_{Z'} = 2000\,GeV$ and $g_1' = 0.290$, $M_{Z'} = 3000$ GeV and $g_1' = 0.435$, with $\mathcal{L} = 1000 fb^{-1}$, respectively.

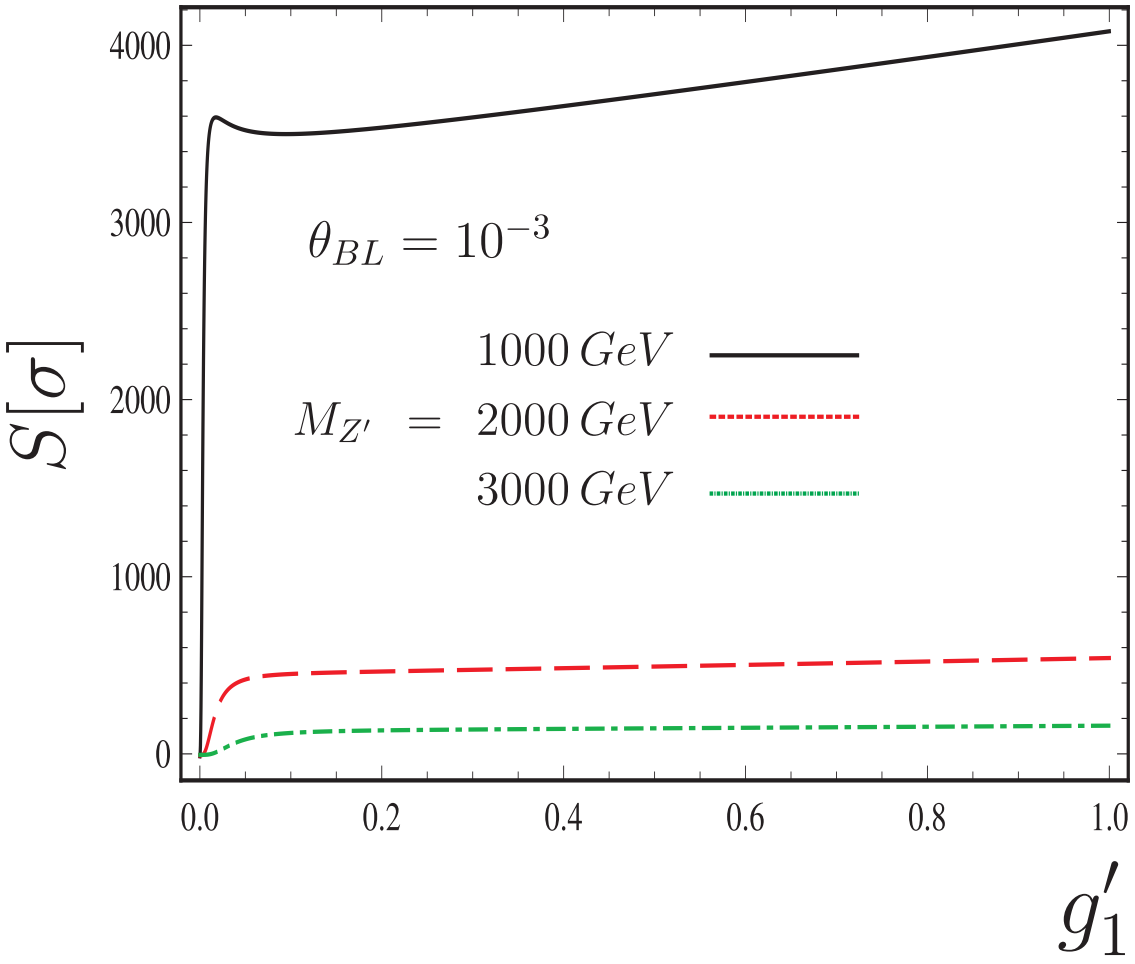

FIG. 8: The statistical significance $S[\sigma]$ of Eq. (41) as a function of g_1'. Starting from the top, the curves are for $M_{Z'} = 1000, 2000, 3000\ GeV$ and $\sqrt{s} = 1000, 2000, 3000\ GeV$ with $\mathcal{L} = 1000\ fb^{-1}$, respectively.

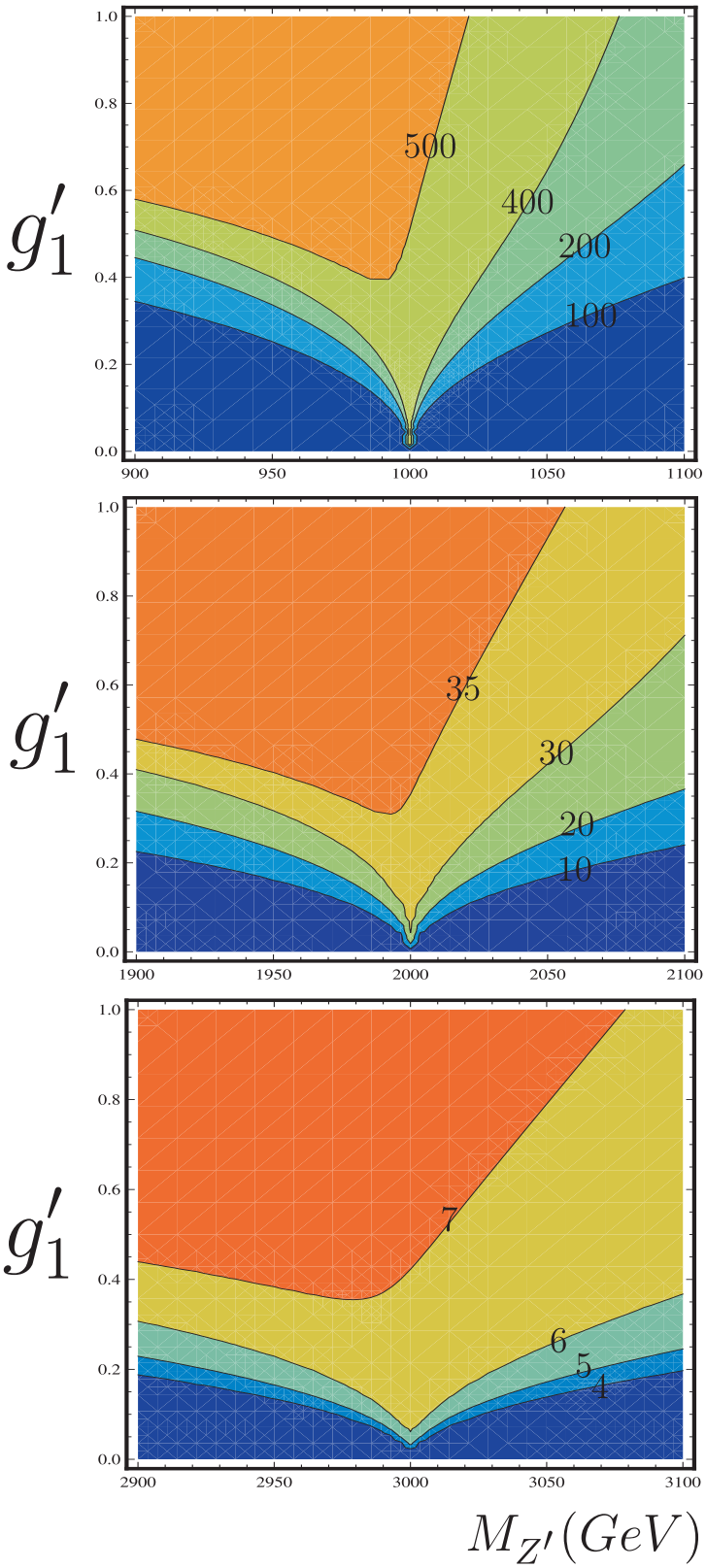

FIG. 9: Correlation between $M_{Z'}$ and g_1'. Top panel: the contours are for $\sigma_{Tot} = 100, 200, 400, 500\ fb$ and $\sqrt{s} = 1000\,GeV$. Central panel: the contours are for $\sigma_{Tot} = 10, 20, 30, 35\ fb$ and $\sqrt{s} = 2000\,GeV$. Bottom panel: the contours are for $\sigma_{Tot} = 4, 5, 6, 7\ fb$ and $\sqrt{s} = 3000\,GeV$.

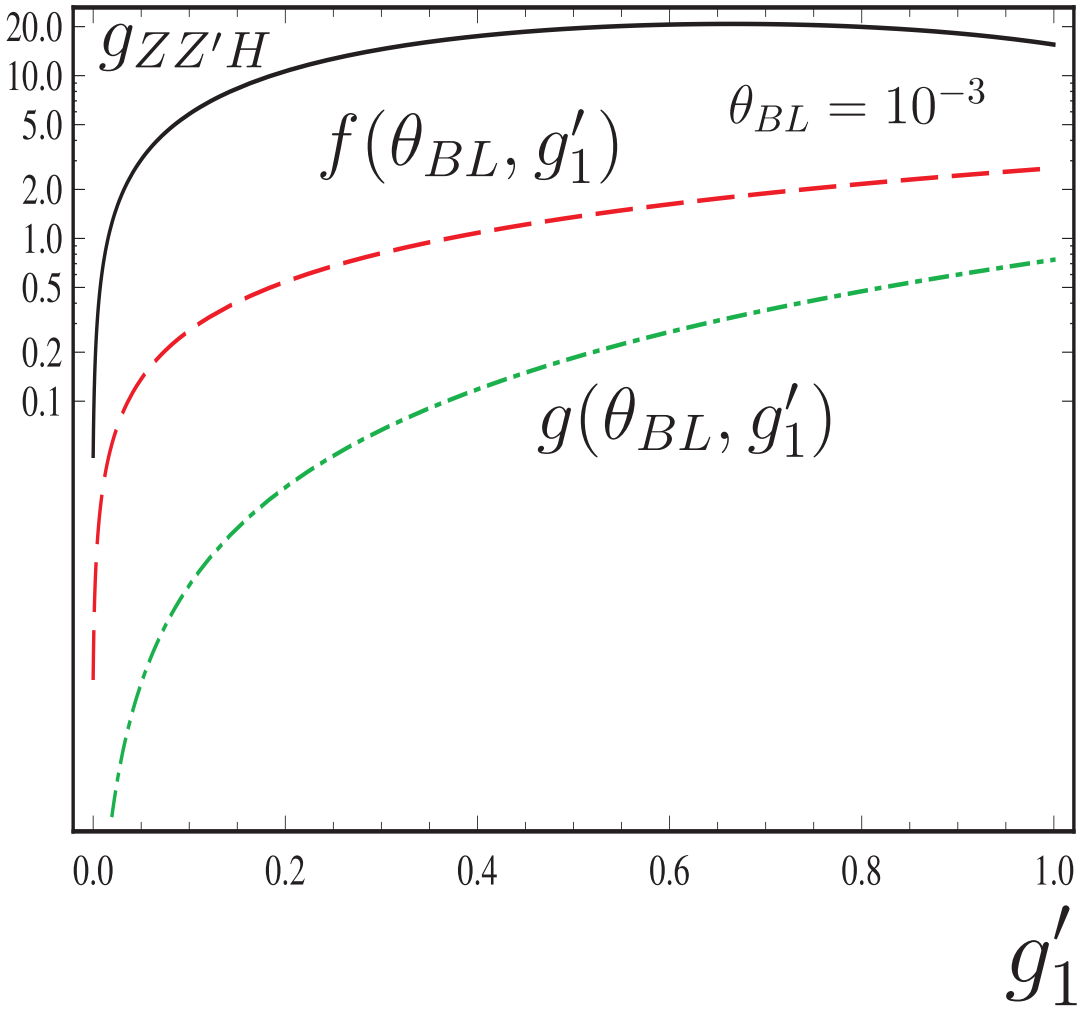

FIG. 10: $g_{ZZ'H}(\theta_{BL}, g_1')$ coupling and $f(\theta_{BL}, g_1')$, $g(\theta_{BL}, g_1')$ functions as a function of g_1', with $\theta_{BL} = 10^{-3}$.

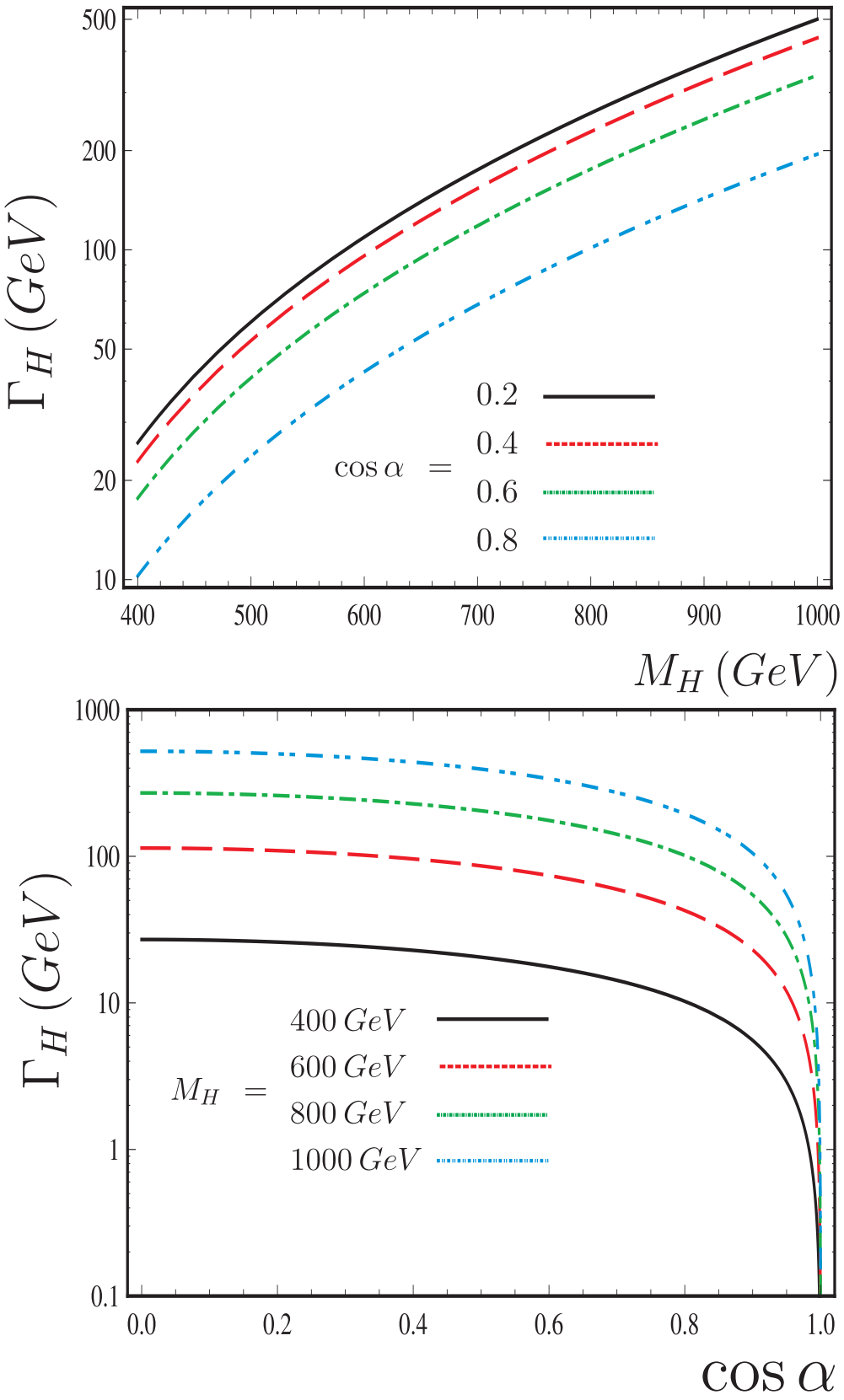

FIG. 11: Top panel: heavy Higgs boson decay width as a function of M_H for $M_h = 125\,GeV$ and $M_{\nu_R} = 300\,GeV$. Bottom panel: heavy Higgs boson decay width as a function of $\cos\alpha$.

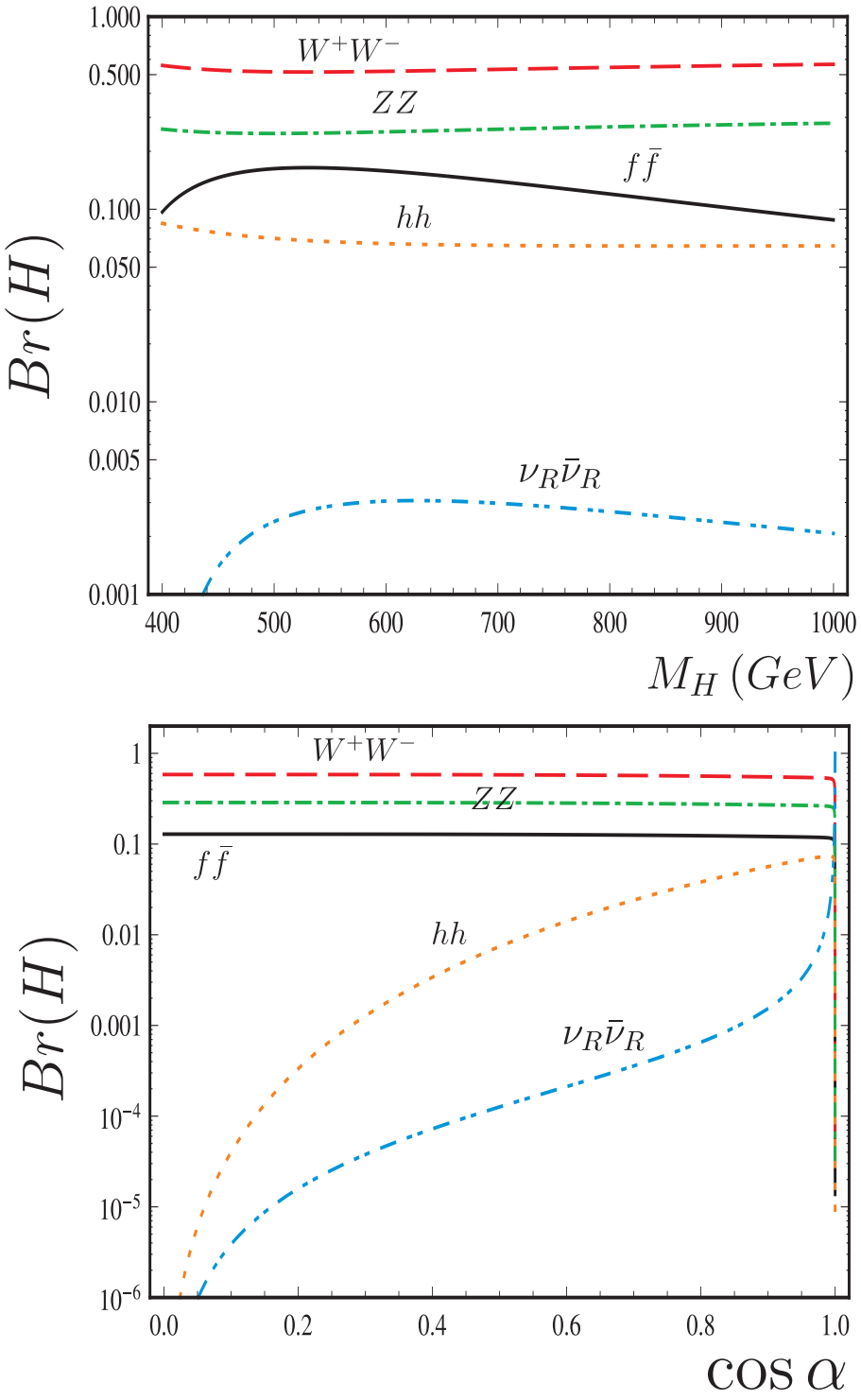

FIG. 12: Top panel: Branching ratios as a function of M_H for $M_h = 125\,GeV$ and $M_{\nu_R} = 300\,GeV$. Bottom panel: Branching ratios as a function of $\cos\alpha$ for $M_h = 125\,GeV$, $M_H = 800\,GeV$ and $M_{\nu_R} = 300\,GeV$.

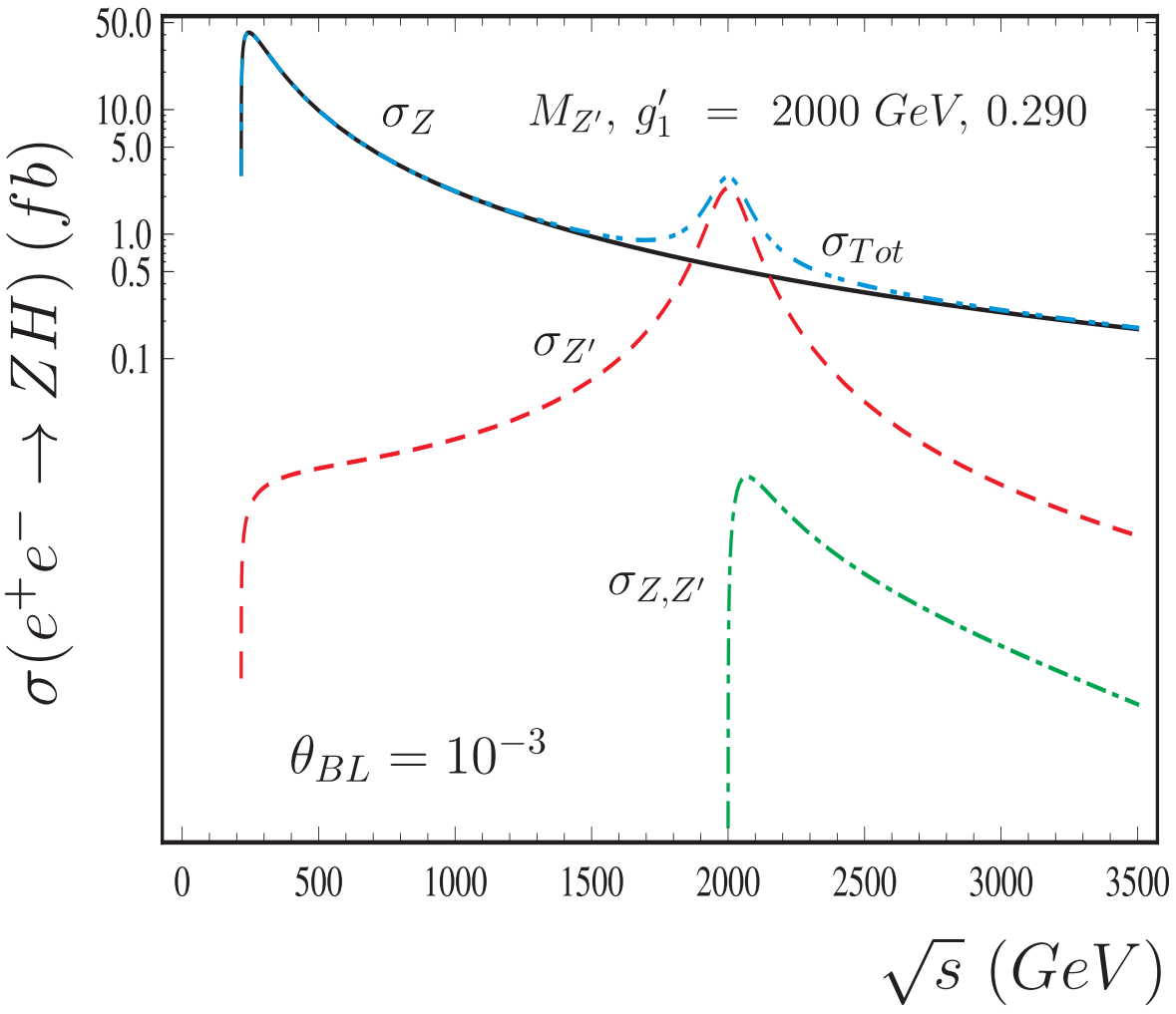

FIG. 13: The cross section of the production process $e^+e^- \to ZH$ as a function of $\sqrt{s}$ for $M_h = 125\ GeV$, $M_H = 800\,GeV$, $M_{Z'} = 2000\,GeV$ and $g_1' = 0.290$. The curves are for $\sigma_Z(e^+e^- \to ZH)$ (Eq. (37)) (solid line), $\sigma_{Z'}(e^+e^- \to ZH)$ (Eq. (38)) (dashed line), $\sigma_{Z,Z'}(e^+e^- \to ZH)$ (Eq. (39)) (dot-dashed line), and the dot dot-dashed line correspond to the total cross section of the process $\sigma_{Tot}(e^+e \to ZH)$ (Eq. (36)), respectively.

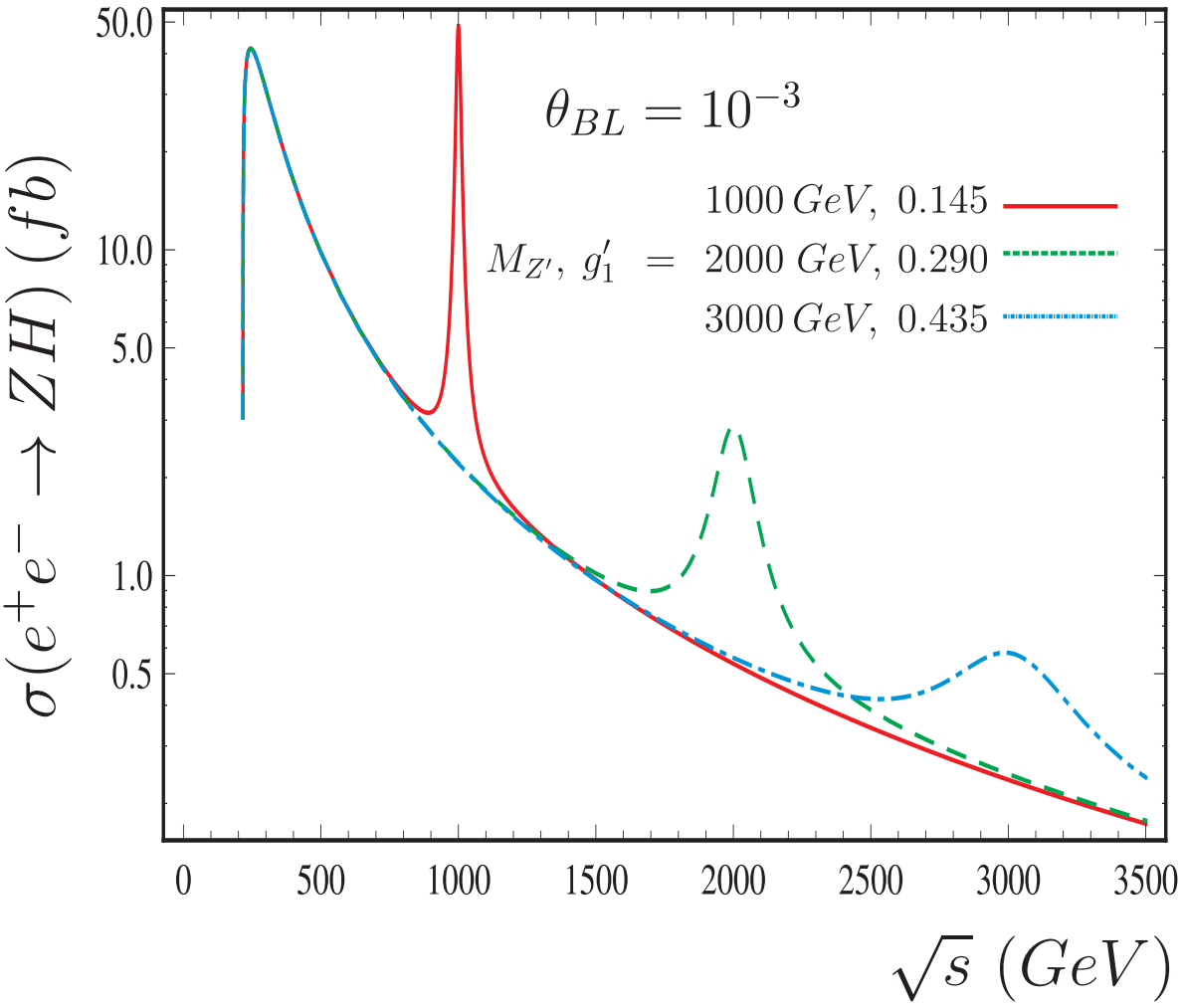

FIG. 14: The total cross section of the production process $e^+e^- \to ZH$ as a function of $\sqrt{s}$ for $M_h = 125\,GeV$ and $M_H = 800\,GeV$. The curves are for $M_{Z'} = 1000\,GeV$ and $g_1' = 0.145$ (solid line), $M_{Z'} = 2000\,GeV$ and $g_1' = 0.290$ (dashed-line), $M_{Z'} = 3000\,GeV$ and $g_1' = 0.435$ (dot-dashed line), respectively.

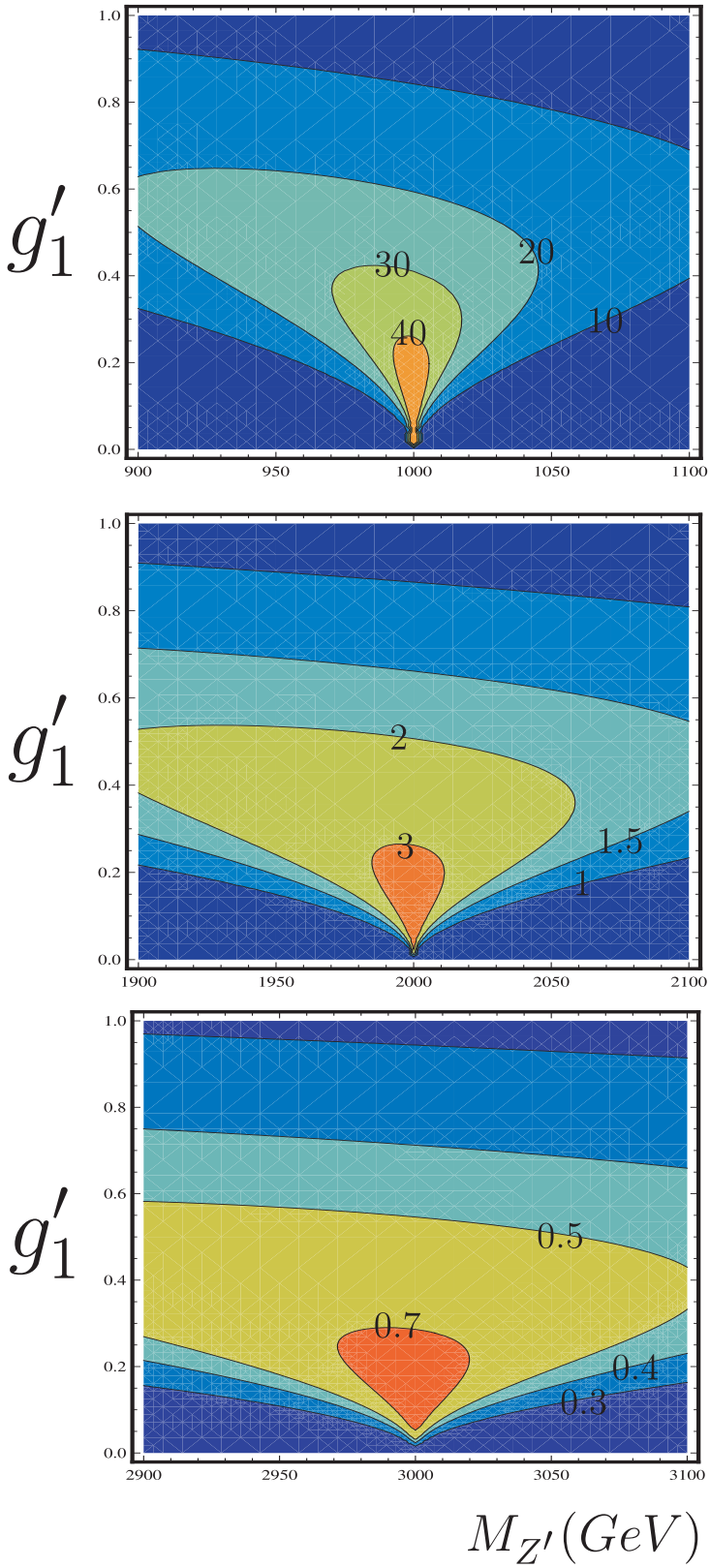

FIG. 15: Correlation between $M_{Z'}$ and g_1'. Top panel: the contours are for $\sigma_{Tot} = 10, 20, 30, 40\ fb$ and $\sqrt{s} = 1000\ GeV$. Central panel: the contours are for $\sigma_{Tot} = 1, 1.5, 2, 3\ fb$ and $\sqrt{s} = 2000\ GeV$. Bottom panel: the contours are for $\sigma_{Tot} = 0.3, 0.4, 0.5, 0.7\ fb$ and $\sqrt{s} = 3000\ GeV$.